nature geoscience

ARTICLES

PUBLISHED ONLINE: 18 SEPTEMBER 2011 | DOI: 10.1038/NGEO1265

Assimilation of upwelled nitrate by small eukaryotes in the Sargasso Sea

Sarah E. Fawcett[1]*, Michael W. Lomas[2], John R. Casey[3], Bess B. Ward[1] and Daniel M. Sigman[1]

Phytoplankton growth is potentially limited by the scarcity of biologically available forms of nitrogen such as nitrate and ammonium. In the subtropical ocean gyres, water column stratification impedes the upward flux of nitrate to surface waters. Phytoplankton in these waters are assumed to rely largely on ammonium and other forms of nitrogen recycled during the breakdown of organic matter. Here, we use flow cytometry to separate prokaryotic and eukaryotic phytoplankton collected from Sargasso Sea surface waters in the summers of 2008 and 2009, and to analyse their respective nitrogen isotope ratios. We show that prokaryotes have a uniformly low ratio of ^{15}N to ^{14}N, $\delta^{15}N$, consistent with their reliance on recycled nitrogen. In contrast, small eukaryotic phytoplankton, less than 30 μm in size, have a higher and more variable $\delta^{15}N$, with a mean value similar to that of nitrate in underlying Subtropical Mode Water. For the summertime Sargasso Sea, we estimate that small eukaryotes obtain more than half of their nitrogen from upwelled nitrate. In addition, our data support the view that sinking material derives largely from eukaryotic, not prokaryotic, phytoplankton biomass.

As an essential nutrient, biologically available nitrogen ('fixed N') has the potential to limit marine productivity and determine phytoplankton community composition. 'New production' is phytoplankton growth in the sunlit upper ocean fuelled by 'new' N: nitrate (NO_3^-) mixed up from the ocean interior, augmented by *in situ* N_2 fixation. Annually, new production balances the export of sinking organic matter from shallow waters, maintaining the sequestration of carbon in the ocean interior[1,2]. In the subtropical ocean, the supply of nitrate from below seems to be slow, such that most phytoplankton growth is thought to be supported by 'recycled' N (refs 3,4) (predominantly ammonium (NH_4^+)).

The Bermuda Atlantic Time-series Study (BATS) site is located at the northern margin of North Atlantic subtropical gyre (the 'Sargasso Sea'), and its summertime conditions are representative of the open subtropical ocean[5]. After higher mixing and productivity in the winter and spring, strong summertime stratification develops at the base of and within the euphotic zone (upper ~100 m; ref. 4), and the wind-mixed surface layer shoals to ≤20 m (ref. 5), resulting in trace nitrate throughout the euphotic zone (Fig. 1a; as low as 0.001–0.01 μM, with sporadic observations of ~0.1 μM; ref. 4). Under these conditions, the recycling of N by euphotic zone biota is thought to be the major N source for phytoplankton growth[1–3].

The photoautotrophic biomass at BATS is comprised of the prokaryotic cyanobacterial genera *Prochlorococcus* and *Synechococcus* (hereafter 'prokaryotes')[6,7] and a number of eukaryotic species (hereafter 'eukaryotes'), predominantly prymnesiophytes and pelagophytes[8]. The N uptake capacities of these different taxa are being investigated (Supplementary Information S3.1), but the low concentrations of all fixed N forms in the Sargasso Sea make it difficult to assess *in situ* N assimilation rates or to determine which taxa (prokaryotes versus eukaryotes) use which N sources.

Nitrogen isotopes in the subtropical ocean

At BATS, N isotope studies have supported the expectation that recycled N fuels most phytoplankton growth. The $\delta^{15}N$ of bulk suspended particulate N (PN) ranges from −3 to 1‰ (refs 9,10), lower than that of nitrate in the underlying Subtropical Mode Water (STMW) ($\delta^{15}N$ of 2–3‰ at 250 m (ref. 11); $\delta^{15}N$, in permil versus atmospheric N_2, $= \{[^{15}N/^{14}N)_{sample}/(^{15}N/^{14}N)_{atm}] - 1\} \times 1{,}000$). Similarly low-$\delta^{15}N$ PN in the Pacific was first interpreted as indicating a substantial input from N_2 fixation[12], which produces N with a $\delta^{15}N$ of −2 to 0‰ (refs 13,14). However, the limited data from BATS indicate that the $\delta^{15}N$ of sinking PN is ~3–4‰ (ref. 9; Fig. 1b), similar to underlying STMW nitrate, suggesting that most of the new N supply is as nitrate from below, with N_2 fixation accounting for only a small fraction of new N input on an annual basis[9]. In this view, the low $\delta^{15}N$ of suspended PN was interpreted as the result of upper ocean N recycling: Zooplankton sustained by upper ocean PN metabolize and excrete ^{15}N-depleted ammonium, the assimilation of which renders phytoplankton low in $\delta^{15}N$ (refs 15,16).

Flow cytometry with nitrogen isotope analysis

Most isotope studies have measured surface ocean PN as a homogenous N pool, but PN includes biologically distinct N-containing particles: diverse living autotrophs and heterotrophs as well as detrital organic matter[17]. By combining flow cytometry with new, high-sensitivity methods for N isotope analysis (the 'persulphate/denitrifier' method[11]), we have characterized the N concentration ([N]) and $\delta^{15}N$ of taxonomically distinct components of the PN suspended in Sargasso Sea surface waters. Samples were collected through the summertime euphotic zone near the BATS site in July 2008 and 2009 (Methods and Supplementary Information S1–S2). Averaging over the euphotic zone, photoautotrophic contribution to bulk PN was 47 ± 9%, consistent with previous findings for particulate carbon[8], and the sorted fractions of *Prochlorococcus*, *Synechococcus* and eukaryotic phytoplankton each comprised roughly a third of photoautotrophic biomass N (Fig. 2a,c).

The $\delta^{15}N$ of bulk PN ranged from −2 to 0‰ (Fig. 2b,d), similar to previous data interpreted as indicating a system supported by recycled N (refs 9,10). The $\delta^{15}N$ of *Prochlorococcus* (−4 to

[1]Princeton University, Department of Geosciences, Guyot Hall, Princeton, New Jersey 08544, USA, [2]Bermuda Institute of Ocean Sciences, St George's GE01, Bermuda, [3]School of Ocean and Earth Science and Technology, University of Hawaii, Honolulu, Hawaii 96822, USA. *e-mail: sfawcett@princeton.edu.

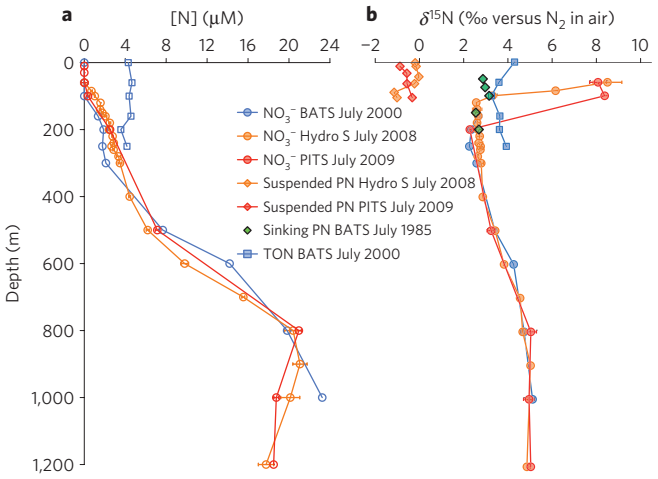

Figure 1 | Important forms of nitrogen in the Sargasso Sea. Depth profiles of summertime N concentrations (**a**) and their corresponding $\delta^{15}N$ values (**b**). **a**, Open circles: [NO_3^-] from BATS July 2000 (blue)[11], Hydrostation S July 2008 (orange, this study), PITS July 2009 (red, this study). Blue squares: [TON] (total organic N, or DON plus the small PN pool) at BATS July 2000 (ref. 11). **b**, Nitrate $\delta^{15}N$ (shaded circles), TON $\delta^{15}N$ (shaded squares), bulk suspended PN $\delta^{15}N$ from Hydrostation S July 2008 (orange diamonds) and PITS July 2009 (red diamonds), $\delta^{15}N$ of sinking PN (green diamonds) from sediment traps at BATS July 1985 (ref. 9). Error bars indicate ±1 standard error of all measurements, including samples from duplicate Niskin bottles, duplicate samples from the same Niskin bottle, and replicate sample analyses.

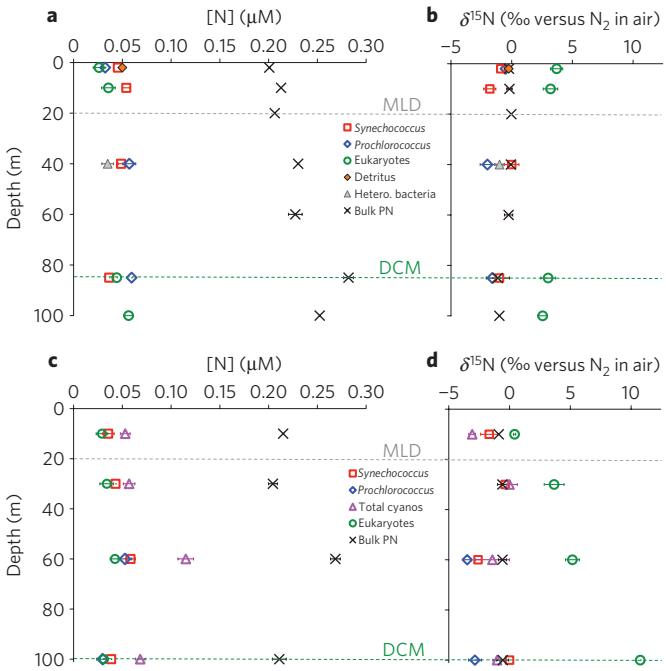

Figure 2 | Abundances and nitrogen isotope ratios of populations sorted by flow cytometry. [N] and $\delta^{15}N$ of flow cytometrically sorted components of the PN from the Sargasso Sea in July 2008 (**a** and **b**) and 2009 (**c** and **d**). The mixed layer depth (MLD; dashed grey line) was ~20 m in both years, and the deep chlorophyll maximum (DCM; dashed green line) was ~85 m in 2008 and ~100 m in 2009. 'Total cyanos' (purple triangles) represents a combined population of *Prochlorococcus* plus *Synechococcus*, sorted and measured independently of the individual genera. 'Detritus' (orange diamonds) denotes dead material (containing no chlorophyll fluorescence or stainable DNA), and 'hetero. bacteria' (grey triangles) refers to heterotrophic bacteria (containing no naturally fluorescing chlorophyll but stainable DNA). Error bars indicate the full range for replicate samples, commonly duplicates, collected, sorted, and analysed independently.

−1‰; Fig. 2b,d) and *Synechococcus* (−3 to −1‰; Fig. 2b,d) was typically slightly lower than that of bulk PN, consistent with the expectation that prokaryotic phytoplankton use recycled N (NH_4^+ and/or simple organic N forms such as amino acids) as their dominant N source throughout the subtropical euphotic zone. Some amount of the prokaryote N supply may derive from N_2 fixation, although only via recycling, as these taxa apparently cannot fix N_2 (ref. 18). Remarkably, the $\delta^{15}N$ of sorted eukaryotes (Fig. 2b,d) was always higher than bulk $\delta^{15}N$ and prokaryote $\delta^{15}N$, typically by >3‰, pointing to a biogeochemical difference between prokaryotes and eukaryotes.

Possible explanations for high eukaryote $^{15}N/^{14}N$

One set of hypotheses for the high eukaryote $\delta^{15}N$ involves the loss of low-$\delta^{15}N$ N from these phytoplankton, such as via the excretion of NO_2^- or NH_4^+. In this N-depleted euphotic zone, autotrophic N excretion seems unlikely (Supplementary Information S3.2.1–S2). Regardless, NO_2^- efflux does not have the required isotopic effect (Supplementary Information S3.2.1). With respect to NH_4^+ release (for instance, in the case of mixotrophy by eukaryotes), heterotrophic bacteria are far more likely to excrete NH_4^+ than are autotrophic phytoplankton, as they do not photosynthesize. However, we measure a $\delta^{15}N$ of −1.0‰ for sorted heterotrophic bacteria (see below; Fig. 2b), which is very similar to the $\delta^{15}N$ of cyanobacteria, implying that some small amount of NH_4^+ excretion by the eukaryotic phytoplankton would not significantly increase their biomass $\delta^{15}N$. As yet, no compelling loss-based explanation has been recognized for the high eukaryote $\delta^{15}N$.

We conclude that the eukaryotes are using a high-$\delta^{15}N$ N source, distinct from that supporting prokaryote production. Possible high-$\delta^{15}N$ N sources include dissolved organic nitrogen (DON) and nitrate. DON has a concentration of 4–5 μM (Fig. 1a; ref. 19) and an annual average $\delta^{15}N$ of 3.9‰ (Fig. 1b), similar to mean eukaryote $\delta^{15}N$[11]. However, the high $\delta^{15}N$ of DON itself is best explained by breakdown to simpler N forms (for example, amino acids and NH_4^+) by N isotope discriminating reactions such as peptide hydrolysis and deamination[20–22]. We know of no reason why eukaryotes would be able to consume bulk DON by a non-fractionating mechanism that is unavailable to prokaryotes[18,23,24]. Finally, bulk DON rarely reaches the $\delta^{15}N$ of 5.2‰ observed for eukaryotes at 60 m in 2009, and never approaches 12.7‰, as observed at 100 m (Fig. 2d; ref. 11).

Nitrate could be supplied by *in situ* nitrification (oxidation of recycled NH_4^+ to nitrite and then nitrate) or by upward mixing of STMW nitrate. Nitrification seems to be minor in the euphotic zone near BATS (ref. 25), although some fraction of the very low-level summertime ambient nitrate may derive from it[4]. Any euphotic zone nitrification that does occur is unlikely to produce nitrite or nitrate with a $\delta^{15}N$ consistently higher than that its NH_4^+ substrate, largely because the isotope effect of ammonium assimilation is expected to be lower than that of ammonium oxidation at very low ambient [NH_4^+] (refs 26,27; Supplementary Information S3.2.3). Thus, even if euphotic zone nitrification were significant, the assimilation of its products by eukaryotes does not explain their clear $\delta^{15}N$ elevation relative to prokaryotes.

Assimilation of new nitrate by eukaryotic phytoplankton

The high eukaryote $\delta^{15}N$ most probably derives from 'new' nitrate mixed into the euphotic zone from below. At the typical depth of winter mixing (150–300 m; ref. 5), nitrate $\delta^{15}N$ is 2–3‰ (Fig. 1b). Owing to isotope discrimination during nitrate assimilation, the $\delta^{15}N$ of biomass produced at any given time should be lower than

that of ambient nitrate. This preferential ^{14}N-nitrate assimilation is evident in the elevated nitrate δ^{15}N at the base of the euphotic zone (Fig. 1b; ref. 11). However, the nitrate concentration of $<0.02\,\mu M$ typical of most of the summertime euphotic zone[4] is below the half-saturation constant for nitrate assimilation ($\sim$0.02–0.03 μM; ref. 28), a condition that probably minimizes isotope discrimination during consumption[29]. Moreover, regardless of any variation in this isotope discrimination, as a given increment of nitrate is assimilated, the δ^{15}N of integrated biomass produced from it will converge on the source nitrate δ^{15}N (Supplementary Information S3.3). Thus, assimilation of new nitrate by eukaryotes would imprint them with a higher mean δ^{15}N than if they assimilated only recycled N. Although diatoms have previously been recognized as important nitrate assimilators[30], they are not a significant fraction of the biomass in our collected $<30\,\mu m$ eukaryote pool[5,8,31]; our results indicate a broad tendency among small eukaryotes, which dominate the Sargasso Sea eukaryote population, to assimilate nitrate. The mean cellular sizes of our sorted prokaryotes (particularly *Synechococcus*) and eukaryotes are not highly distinct[8], raising the possibility of a deeper biochemical origin for their N source difference.

Although we do not understand the mechanism controlling this N source difference, there are potential explanations. Given that it is less energetically expensive to assimilate reduced N forms[32], prokaryotic phytoplankton may outcompete eukaryotes for recycled N. Alternatively, eukaryotes may indeed compete successfully for low-level nitrate, perhaps because of their uncoupling of nitrate transport from nitrate reduction (Supplementary Information S3.4). Mechanistic arguments aside, our observation of eukaryotic dominance of nitrate assimilation is consistent with the seasonal pattern of phytoplankton succession in the Sargasso Sea, from eukaryotes after deep winter mixing to *Synechococcus* and then *Prochlorococcus* with intensifying stratification and N depletion into the summer[5,8].

If the collected phytoplankton recorded the entire annual cycle, the δ^{15}N of their nitrate supply would be the concentration-weighted mean δ^{15}N of STMW nitrate down to the depth of winter mixing (2–3‰). However, individual eukaryote cells should integrate over only a period of days, so their nitrate supply has a higher δ^{15}N, best approximated by nitrate at the base of the summertime euphotic zone. At the deep chlorophyll maximum (DCM), nitrate δ^{15}N was 6.2‰ in 2008 and 8.4‰ in 2009 (Fig. 1b; at 85 m and 100 m, and $[NO_3^-]$ of 0.49 μM and 0.36 μM, respectively). The δ^{15}N of a given sample of eukaryotes can be higher than this because the collected cells may have acquired nitrate that has already undergone further δ^{15}N elevation by assimilation in the euphotic zone; this can explain the extraordinarily high δ^{15}N (12.7‰) of the eukaryote sample from 100 m in 2009.

On average, the consumption of the subsurface nitrate supply is likely to progress upward, such that isotope discrimination during nitrate assimilation might be expected to cause higher eukaryote δ^{15}N in shallower samples. Depth variations in the relative importance of nitrate uptake may explain the lack of such an upward δ^{15}N increase in our data, and indeed the opposite trend in 2009: eukaryotes in the surface mixed layer may rely more on recycled N than those below the mixed layer. Alternatively, upper ocean circulation is chaotic, such that a given sampling may capture a time when the mixed layer has a more recently delivered parcel of nitrate-bearing water than the underlying euphotic zone. For instance, the passage of Hurricane Bertha over the BATS site may have affected nutrient supply two weeks before our sampling in July 2008, although the hydrographic, nutrient, and cell abundance data are typical of July climatology. Finally, as noted above, the isotope effect of nitrate assimilation is likely to decrease under very low nitrate concentrations, minimizing the isotopic signal of progressive nitrate assimilation above the DCM. Although continued sampling is required to characterize and understand the variation, the high mean δ^{15}N of our eukaryotes requires nitrate assimilation, regardless of isotope effect (Supplementary Information S3.3).

Our interpretation requires that subsurface nitrate is transported upward into the euphotic zone and even the surface mixed layer, across their underlying summertime thermoclines. This transport may be driven by purely physical mechanisms: hydrographic studies have documented summertime transport of nitrate into the subtropical euphotic zone associated with mesoscale eddies[33] and related phenomena[34]. Biologically facilitated physical transport has also been suggested[35]. Finally, direct biological transport has been demonstrated in some systems[30], and recent data from near Hawaii suggest that this mechanism transports nitrate into the mixed layer[34]. Future work coupling isotope measurements with intensive hydrographic data may distinguish among these processes.

Summertime eukaryote and community *f*-ratios

At an ecosystem level, the relative importance of new versus recycled N for phytoplankton production is traditionally quantified as the '*f*-ratio', the ratio of nitrate assimilation (that is, new production) to total N assimilation[1,2]. Assuming parallel cycling of carbon and N, the *f*-ratio is also the fraction of net primary production resulting in carbon export from the euphotic zone. Given the nutrient-poor conditions at BATS during the summer, a low *f*-ratio is expected[2].

Our δ^{15}N measurements of sorted components of the suspended PN allow a non-incubation approach for estimating the *f*-ratio. An *f*-ratio for each phytoplankton group is estimated from its δ^{15}N, and these are then assembled into a community *f*-ratio (Supplementary Information S3.5). This exercise is highly dependent on the δ^{15}N assigned to new and recycled N. We assume that *Prochlorococcus* and *Synechococcus* together assimilate only recycled N, and we use the δ^{15}N of nitrate at the DCM as a measure of the July nitrate supply to the euphotic zone. The assumptions for these end-members and our exclusion of N_2 fixation as a source of low-δ^{15}N N are chosen to err on the side of underestimating the *f*-ratio (Supplementary Information S3.5).

We calculate eukaryote-specific *f*-ratios of 0.60 and 0.67 for July 2008 and 2009, respectively, and total community *f*-ratios of 0.15 and 0.23. Despite the biases in our calculations to underestimate the *f*-ratio, our community estimates are much higher than those based on comparison of annually integrated primary production and sediment trap-derived organic carbon export at BATS, which imply an annual *f*-ratio of 0.06 and a still lower summertime value[5]. Our estimates are lower than the highest annual estimates derived from geochemical tracers (0.36 ± 0.12; ref. 36; Supplementary Information S3.5), but July is the most nutrient-poor period at BATS, when the lowest *f*-ratio is expected[1,2,4], and thus our summer estimates support the geochemically derived annual *f*-ratio estimates.

Nitrogen isotopes of other sorted samples

In July 2008, a heterotrophic bacterial population sorted from 40 m contributed 0.035 μM N ($\sim$15% of bulk PN) with a δ^{15}N of −1.0‰, whereas detrital material from the surface comprised 0.05 μM N ($\sim$25% of bulk PN), with a δ^{15}N of −0.3‰ (Fig. 2a,b). The similarity of heterotrophic bacteria to cyanobacterial δ^{15}N suggests that bacteria also assimilate predominantly recycled N. The recycled N consumed by the bacteria is probably in the form of simple organic compounds liberated during their extracellular degradation of organic matter[37]. The δ^{15}N of detritus suggests that it derives largely from prokaryotic phytoplankton and/or heterotrophic bacteria, which is consistent with the dominance of these combined N pools relative to eukaryotes and with the expectation that prokaryotic phytoplankton preferentially enter the microbial loop[38]. The minimal δ^{15}N elevation in the detrital pool implies that isotope fractionation during degradation typically

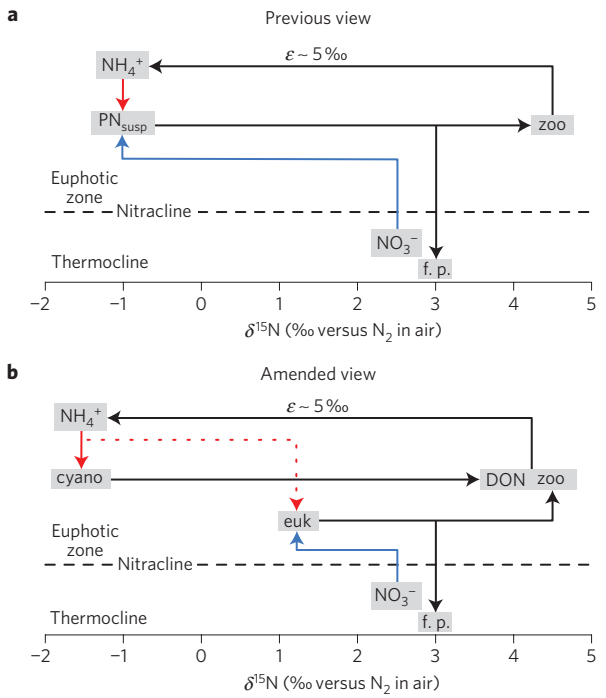

Figure 3 | Changes to our view of Sargasso Sea nitrogen cycling. Previously understood mean annual view of N fluxes and their δ^{15}N in the surface of the Sargasso Sea (**a**) and our amended view (**b**). Blue arrows represent the new N source (subsurface nitrate, δ^{15}N of 2–3‰); red arrows show recycled N (mostly ammonium); red dashed arrow indicates that eukaryotes get less of their N from recycled sources than from new nitrate. 'PN_{susp}' refers to bulk suspended PN, 'cyano' to prokaryotic phytoplankton, 'euk' to eukaryotic phytoplankton, 'DON' to dissolved organic nitrogen, 'zoo' to herbivorous copepod zooplankton, and 'f.p.' to faecal pellets produced by them, approximating export. For comparison with **a**, we extrapolate our July findings to an annual average, so as to use the same nitrate supply δ^{15}N. Thus, eukaryote δ^{15}N in **b** reflects its observed position relative to new nitrate and recycled N sources, rather than the measured July eukaryote δ^{15}N. This schematic neglects N_2 fixation, which has been estimated to represent a small fraction of the annual N supply to the BATS euphotic zone[9,11].

occurs after organic matter has been solubilized to DON, such that isotopic elevation occurs in DON and not PN (refs 11,22).

The $^{15}N/^{14}N$ of sinking and suspended particles

The traditional view of N fluxes in the Sargasso Sea (Fig. 3a) has been that the export of high-δ^{15}N zooplankton faecal material from the euphotic zone balances the δ^{15}N of the STMW nitrate supply. In this view, the preferential excretion of ^{14}N-rich recycled N during heterotrophic metabolism lowers the δ^{15}N of bulk PN relative to the subsurface nitrate supply. However, work to date indicates that the δ^{15}N of faecal pellets is not as elevated as the zooplankton producing them[39] and may instead resemble the δ^{15}N of the food source[40,41]. Thus, it is unclear how the consumption by herbivorous zooplankton of bulk suspended PN with a δ^{15}N of ~ −2–0‰ could yield the export flux δ^{15}N of 3–4‰ measured near BATS (ref. 9).

The δ^{15}N of sorted eukaryotes averaged over the euphotic zone was 3.0‰ in 2008 and 5.0‰ in 2009, with a mean δ^{15}N similar to the previously measured sinking flux. Sinking flux δ^{15}N is therefore consistent with faecal pellets produced by zooplankton that have preferentially consumed eukaryotic phytoplankton, without the need for an unrealistically large δ^{15}N increase (~5‰) during the passage of phytoplankton biomass N through the zooplankton gut (Fig. 3b). Indeed, studies indicate selective feeding by herbivorous zooplankton on phytoplankton size classes dominated by eukaryotes[42,43]. A simple isotope-driven end-member mixing calculation indicates that *Prochlorococcus* and *Synechococcus* contribute less than half (roughly a third) of sinking PN or carbon[44] (Supplementary Information S3.6), despite the importance of prokaryotes at BATS (>65% of photoautotrophic biomass N in this study). Thus, our data suggest that the eukaryotic phytoplankton contribution to export is disproportionately larger than their contribution to total net primary production, a long-held view[45] that has recently been challenged[46]. Given that export production drives carbon sequestration in the ocean interior, and that this study was conducted in a region where prokaryotic phytoplankton are as dominant as anywhere in the ocean, our results suggest that the biological pump in nutrient-poor subtropical gyres (~60% of oceanic surface area) is driven mostly by eukaryotic phytoplankton. With regard to paleoceanographic studies, our data indicate a disconnect between prokaryote-dominated biomass in the low-latitude surface ocean and the organic matter sinking to the seabed, which we find to be predominantly of eukaryotic origin. Although small eukaryotes dominate the Sargasso Sea eukaryote pool[5,8,31], previous work suggests that the large eukaryotes also assimilate nitrate and are preferentially incorporated into sinking particles[30,45], indicating the same eukaryotic dominance of the sinking flux in more productive ocean regions as well.

Our data suggest that small eukaryotic phytoplankton are more readily removed to the deep ocean than are cyanobacteria. The PN that sinks into the deep ocean is remineralized to nitrate, which is eventually resupplied to surface waters. We have also found that the eukaryotes are more reliant on the subsurface nitrate supply, whereas the prokaryotes are more completely recycled within the surface ocean and, in turn, rely mostly on the N forms recycled there (for example, NH_4^+). The internal consistency between uptake and remineralization in each group raises the possibility that the N uptake strategy of a given phytoplankton group is partially guided by the fate of its biomass.

Methods

Field collections. Samples were collected aboard the R/V *Atlantic Explorer* at Hydrostation S (32° 10′ N, 64° 34′ W) on cruise HS1113 in July 2008 and at PITS station (31° 35′ N, 64° 10′ W) on BATS cruise B248 in July 2009. Seawater was collected for PN and nitrate (NO_3^-) at the surface, 10 m, 40 m, 85 m and 100 m in 2008; and 10 m, 30 m, 60 m, and 100 m in 2009. Five 12 l Niskin bottles were tripped at each depth to collect sufficient PN for later isotope analysis. Additional Niskin bottles were tripped at regular intervals from below the euphotic zone down to 1,000 m (see Supplementary Information S1.1) and subsampled for later measurement of [NO_3^-] and NO_3^- δ^{15}N. For PN collections, 8 l of seawater from each of the shallower Niskin bottles was passed through a 47 mm 0.4 µm polycarbonate filter under gentle vacuum filtration. Filters were stored in 5 ml acid-washed cryovials with ~4 ml of 0. 2 µm pre-filtered seawater and 200 µl of 10% formaldehyde solution (see Supplementary Information S1.1 and S1.2), then flash frozen for later flow cytometric sorting. In 2008, bulk PN was collected by filtering 8 l seawater aliquots onto precombusted glass fibre filters; total N content and δ^{15}N was analysed with an elemental analyser (NC2500 Carlo Erba) interfaced through a ConFlo III with a ThermoFischer Scientific DeltaPlusXL mass spectrometer. In 2009, bulk PN was collected on 0.4 µm polycarbonate filters and processed in the same manner as sorted samples.

Flow cytometric sorting. Samples were thawed and agitated to quantitatively remove fixed cells from the filters (recoveries were >95%, Supplementary Information S1.2.1), and the resuspended cells were then filtered through a 30 µm mesh to remove any large particles or chains of cells that could clog the flow cytometer sorting tip. Samples were sorted for *Prochlorococcus*, *Synechococccus*, eukaryotic algae, heterotrophic bacteria, and 'detritus'. Autotrophs were identified and sorted unstained according to ref. 47 (see Supplementary Information S1.2.2). A pool of heterotrophs containing bacteria and archaea (hereafter simply 'bacteria') were identified by nucleic acid staining with the cyanine dye SYBR Green I (Invitrogen, Carlsbad, CA) and gated with side scatter, green fluorescence (relative nucleic acid content; 530/40 nm), and red fluorescence to discriminate low nucleic acid content heterotrophic bacteria from *Prochlorococcus*. 'Detritus' was defined as non-fluorescing small particles in SYBR Green stained samples. All post-acquisition analysis was performed using FCS Express (DeNovo Software, Los Angeles, CA).

A high-speed jet-in-air Influx Cell Sorter (Cytopeia, Seattle, WA) was used for all analysis and sorts. A 100 mW blue (488 nm) laser (Coherent, Santa Clara, CA) run at full power was used for excitation of SYTO-13 stained and autofluorescent cells (see Supplementary Information S1.2.3 for sort conditions). With these sort conditions and event rates kept below 2×10^4 s^{-1}, software abort rates were <1%, sort purity was better than 95%, and mean recovery from secondary sorts was 98.1 ± 1.1%. Sorted cells were deposited gently into 5 ml polystyrene Falcon tubes (BD Biosciences, San Jose, CA).

Oxidation of organic N to NO_3^-. Sorted cell populations were filtered onto 25 mm 0.2 μm polycarbonate filters by gentle vacuum filtration. Both sorted and bulk PN filters were placed in combusted 12 ml Wheaton vials and 1–2 ml of ultra-high purity deionized water was added. Vials were sonicated for 60 min to dislodge cells from filters into the deionized water, after which filters were removed. Cellular N content and δ^{15}N were measured by coupling persulphate oxidation of organic N to NO_3^- with chemiluminescent analysis and the 'denitrifier method'[11] (see Supplementary Information S1.2.4). The final N content and δ^{15}N of these samples was corrected for the N blank associated with the reagents. N content was converted to N concentration ([N]) using the seawater volume filtered for each PN sample, corrected for volume loss during flow cytometry (see Supplementary Information S2 for methods validation).

Water column [NO_3^-] and nitrate δ^{15}N. Water samples were collected for [NO_3^-] from the surface to 1,000 m and for δ^{15}N of NO_3^- from 60 m to 1,000 m at Hydrostation S in 2008 and PITS in 2009. [NO_3^-] was determined by reduction to nitric oxide followed by nitric oxide measurement with a chemiluminescent detector[48] (Teledyne model #200 EU), in a configuration with a detection limit of ~0.025 μM.

The δ^{15}N of NO_3^- was measured using the 'denitrifier method'[49] for quantitative bacterial conversion of nitrate to nitrous oxide followed by the isotopic analysis of the nitrous oxide product. The isotopic composition of the nitrous oxide was measured by gas chromatography-isotope ratio mass spectrometry using a modified ThermoFinnigan GasBench II and DeltaPlus[50] (see Supplementary Information S1.2.5).

Received 4 October 2010; accepted 16 August 2011; published online 18 September 2011

References

1. Dugdale, R. C. & Goering, J. J. Uptake of new and regenerated forms of nitrogen in primary production. *Limnol. Oceanogr.* **12,** 196–206 (1967).
2. Eppley, R. W. & Peterson, B. J. Particulate organic matter flux and planktonic new production in the deep ocean. *Nature* **282,** 677–680 (1979).
3. Menzel, D. W. & Ryther, J. H. The annual cycle of primary production in the Sargasso Sea off Bermuda. *Deep-Sea Res.* **6,** 351–367 (1960).
4. Lipschultz, F. A time-series assessment of the nitrogen cycle at BATS. *Deep-Sea Res. II* **48,** 1897–1924 (2001).
5. Steinberg, D. K. *et al.* Overview of the US JGOFS Bermuda Atlantic Time-series Study (BATS): A decade-scale look at ocean biology and biogeochemistry. *Deep-Sea Res. II* **48,** 1405–1447 (2001).
6. Chisholm, S. W. *et al.* novel free-living prochlorophyte abundant in the oceanic euphotic zone. *Nature* **334,** 340–343 (1988).
7. Waterbury, J. B., Watson, S., Guillard, R. R. L. & Brand, L. E. Widespread occurrence of a unicellular, marine, planktonic, cyanobacterium. *Nature* **277,** 293–294 (1979).
8. DuRand, M. D., Olson, R. J. & Chisholm, S. W. Phytoplankton population dynamics at the Bermuda Atlantic Time-series station in the Sargasso Sea. *Deep-Sea Res. II* **48,** 1983–2003 (2001).
9. Altabet, M. A. Variations in nitrogen isotopic composition between sinking and suspended particles: Implications for nitrogen cycling and particle transformation in the open ocean. *Deep-Sea Res.* **35,** 535–554 (1988).
10. Altabet, M. A. A time-series study of the vertical structure of nitrogen and particle dynamics in the Sargasso Sea. *Limnol. Oceanogr.* **34,** 1185–1201 (1989).
11. Knapp, A. N., Sigman, D. M. & Lipschultz, F. N isotopic composition of dissolved organic nitrogen and nitrate at the Bermuda Atlantic Time-series Study site. *Glob. Biogeochem. Cycles* **19,** 1–15 (2005).
12. Saino, T. & Hattori, A. Geographical variation of the water column distribution of suspended particulate organic nitrogen and its ^{15}N natural abundance in the Pacific and its marginal seas. *Deep-Sea Res. I* **34,** 807–827 (1987).
13. Carpenter, E. J., Harvey, H. R., Fry, B. & Capone, D. G. Biogeochemical tracers of the marine cyanobacterium *Trichodesmium*. *Deep-Sea Res. I* **44,** 27–38 (1997).
14. Minagawa, M. & Wada, E. Nitrogen isotope ratios of red tide organisms in the East China Sea—a characterization of biological nitrogen-fixation. *Mar. Chem.* **19,** 245–259 (1986).
15. Checkley, D. M. Jr & Miller, C. A. Nitrogen isotope fractionation by oceanic zooplankton. *Deep-Sea Res.* **36,** 1449–1456 (1989).
16. Montoya, J. P., Carpenter, E. J. & Capone, D. G. Nitrogen fixation and nitrogen isotope abundances in zooplankton of the oligotrophic North Atlantic. *Limnol. Oceanogr.* **47,** 1617–1628 (2002).
17. Rau, G. H., Teyssie, J. L., Rassoulzadegan, F. & Fowler, S. W. ^{13}C/^{12}C and ^{15}N/^{14}N variations among size-fractionated marine particles—implications for their origin and trophic relationships. *Mar. Ecol.-Prog. Ser.* **59,** 33–38 (1990).
18. Moore, L. R., Post, A. F., Rocap, G. & Chisholm, S. W. Utilization of different nitrogen sources by the marine cyanobacteria *Prochlorococcus* and *Synechococcus*. *Limnol. Oceanogr.* **47,** 989–996 (2002).
19. Hansell, D. A. & Carlson, C. A. Biogeochemistry of total organic carbon and nitrogen in the Sargasso Sea: Control by convective overturn. *Deep-Sea Res. II* **48,** 1649–1667 (2001).
20. Macko, S. A., Estep, M. L. F., Engel, M. H. & Hare, P. E. Kinetic fractionation of stable nitrogen isotopes during amino-acid transamination. *Geochim. Cosmochim. Acta* **50,** 2143–2146 (1986).
21. Silfer, J. A., Engel, M. H. & Macko, S. A. Kinetic fractionation of stable carbon and nitrogen isotopes during peptide-bond hydrolysis—experimental evidence and geochemical implications. *Chem. Geol.* **101,** 211–221 (1992).
22. Knapp, A. N., Sigman, D. M., Lipschultz, F., Kustka, A. & Capone, D. G. Interbasin isotopic correspondence between upper-ocean bulk DON and subsurface nitrate and its implications for marine nitrogen cycling. *Glob. Biogeochem. Cycles.* (in the press).
23. Zubkov, M. V., Fuchs, B. M., Tarran, G. A., Burkill, P. H. & Amann, R. High rate of uptake of organic nitrogen compounds by *Prochlorococcus* cyanobacteria as a key to their dominance in oligotrophic oceanic waters. *Appl. Environ. Microbiol.* **69,** 1299–1304 (2003).
24. Wawrik, B., Callaghan, A. V. & Bronk, D. A. Use of inorganic and organic nitrogen by *Synechococcus spp.* and diatoms on the West Florida shelf as measured using stable isotope probing. *Appl. Environ. Microbiol.* **75,** 6662–6670 (2009).
25. Lomas, M. W. & Lipschultz, F. Forming the primary nitrite maximum: Nitrifiers or phytoplankton. *Limnol. Oceanogr.* **51,** 2453–2467 (2006).
26. Hoch, M. P., Fogel, M. L. & Kirchman, D. L. Isotope fractionation associated with ammonium uptake by a marine bacterium. *Limnol. Oceanogr.* **37,** 1447–1459 (1992).
27. DiFiore, P. J., Sigman, D. M. & Dunbar, R. B. Upper ocean nitrogen fluxes in the Polar Antarctic Zone: Constraints from the nitrogen and oxygen isotopes of nitrate. *Geochem. Geophys. Geosyst.* **10,** Q11016 (2009).
28. Harrison, W. G., Harris, L. R. & Irwin, B. D. The kinetics of nitrogen utilization in the oceanic mixed layer: Nitrate and ammonium interactions at nanomolar concentrations. *Limnol. Oceanogr.* **41,** 16–32 (1996).
29. Granger, J., Sigman, D. M., Lehmann, M. F. & Tortell, P. D. Nitrogen and oxygen isotope fractionation during dissimilatory nitrate reduction by denitrifying bacteria. *Limnol. Oceanogr.* **53,** 2533–2545 (2008).
30. Villareal, T. A. *et al.* Upward transport of oceanic nitrate by migrating diatom mats. *Nature* **397,** 423–425 (1999).
31. Goericke, R. Response of phytoplankton community structure and taxon-specific growth rates to seasonally varying physical forcing in the Sargasso Sea off Bermuda. *Limnol. Oceanogr.* **43,** 921–935 (1998).
32. Cochlan, W. P. & Harrison, P. J. Inhibition of nitrate uptake by ammonium and urea in the eucaryotic picoflagellate *Micromonas pusilla* (Butcher) Manton et Parke. *J. Exp. Mar. Biol. Ecol.* **153,** 143–152 (1991).
33. McGillicuddy, D. J. Jr *et al.* Influence of mesoscale eddies on new production in the Sargasso Sea. *Nature* **394,** 263–266 (1998).
34. Johnson, K. S., Riser, S. C. & Karl, D. M. Nitrate supply from the deep to near-surface waters of the North Pacific subtropical gyre. *Nature* **465,** 1062–1065 (2010).
35. Katija, K. & Dabiri, J. O. A viscosity-enhanced mechanism for biogenic ocean mixing. *Nature* **460,** 624–626 (2009).
36. Jenkins, W. J. Studying subtropical thermocline ventilation and circulation using tritium and ^{3}He. *J. Geophys. Res.* **103,** 15817–15831 (1998).
37. Fenchel, T., King, G. M. & Blackburn, T. H. *Bacterial Biogeochemistry: The Ecophysiology of Mineral Cycling* (Elsevier Academic Press, 1998).
38. Ducklow, H. W., Purdie, D. A., Williams, P. J. L. & Davies, J. M. Bacterioplankton—a sink for carbon in a coastal marine plankton community. *Science* **232,** 865–867 (1986).
39. Altabet, M. A. & Small, L. F. Nitrogen isotopic ratios in fecal pellets produced by marine zooplankton. *Geochim. Cosmochim. Acta* **54,** 155–163 (1990).
40. Montoya, J. P., Wiebe, P. H. & McCarthy, J. J. Natural abundance of ^{15}N in particulate nitrogen and zooplankton in the Gulf Stream region and warm-core ring 86a. *Deep-Sea Res. I* **39,** S363–S392 (1992).
41. Tamelander, T., Soreide, J. E., Hop, H. & Carroll, M. L. Fractionation of stable isotopes in the Arctic marine copepod *Calanus glacialis*: Effects on the isotopic composition of marine particulate organic matter. *J. Exp. Mar. Biol. Ecol.* **333,** 231–240 (2006).
42. Harbison, G. R. & McAlister, V. L. Filter-feeding rates and particle retention efficiencies of 3 species of *Cyclosalpa* (Tunicata, Thaliacea). *Limnol. Oceanogr.* **24,** 875–892 (1979).

43. Schnetzer, A. & Steinberg, D. K. Natural diets of vertically migrating zooplankton in the Sargasso Sea. *Mar. Biol.* **141,** 403 (2002).
44. Lomas, M. W. & Moran, S. B. Evidence for aggregation and export of cyanobacteria and nano-eukaryotes from the Sargasso Sea euphotic zone. *Biogeosciences* **8,** 203–216 (2011).
45. Michaels, A. F. & Silver, M. W. Primary production, sinking fluxes and the microbial food web. *Deep-Sea Res.* **35,** 473–490 (1988).
46. Richardson, T. L. & Jackson, G. A. Small phytoplankton and carbon export from the surface ocean. *Science* **315,** 838–840 (2007).
47. Casey, J. R. *et al*. Phytoplankton taxon-specific orthophosphate (Pi) and ATP utilization in the western subtropical North Atlantic. *Aquat. Microbial. Ecol.* **58,** 31–44 (2009).
48. Braman, R. S. & Hendrix, S. A. Nanogram nitrite and nitrate determination in environmental and biological materials by vanadium(III) reduction with chemiluminescence detection. *Anal. Chem.* **61,** 2715–2718 (1989).
49. Sigman, D. M. *et al*. A bacterial method for the nitrogen isotopic analysis of nitrate in seawater and freshwater. *Anal. Chem.* **73,** 4145–4153 (2001).
50. Casciotti, K. L., Sigman, D. M., Hastings, M. G., Böhlke, J. K. & Hilkert, A. Measurement of the oxygen isotopic composition of nitrate in seawater and freshwater using the denitrifier method. *Anal. Chem.* **74,** 4905–4912 (2002).

Acknowledgements

We thank A. Babbin, S. Bell, J. Granger, A. Knapp, H. Ren and L. Treibergs, the staff of the Bermuda Institute of Ocean Sciences and the captain and crew of the R/V *Atlantic Explorer*. We also thank B. Plessen at GeoForschungsZentrum, Potsdam, for analysis of bulk PN samples from July 2008. N. Levine pointed us towards the possible impacts of Hurricane Bertha. This work was supported by the Charrock Foundation, by the Siebel Energy Grand Challenge of Princeton University, and by the US NSF through grants OCE-0752161 (M.W.L.), OCE-0452162 (B.B.W.) and OCE-0447570 (D.M.S.). This is BIOS contribution no. 2028.

Author contributions

M.W.L. and D.M.S. suggested the research area, S.E.F., M.W.L., B.B.W. and D.M.S. planned the project, S.E.F. and J.R.C. performed most of the work, and all authors wrote the paper, led by S.E.F.

Additional information

The authors declare no competing financial interests. Supplementary information accompanies this paper on www.nature.com/naturegeoscience. Reprints and permissions information is available online at http://www.nature.com/reprints. Correspondence and requests for materials should be addressed to S.E.F.

nature geoscience

SUPPLEMENTARY INFORMATION

DOI: 10.1038/NGEO1265

Assimilation of upwelled nitrate by small eukaryotes in the Sargasso Sea

Sarah E. Fawcett,* Michael W. Lomas, John R. Casey, Bess B. Ward and Daniel M. Sigman

*Corresponding author: sfawcett@princeton.edu

1. Supplemental Materials and Methods

We developed a novel protocol to analyze the $\delta^{15}N$ of taxon-specific groups from marine particles collected by gentle vacuum filtration. The protocol includes 1) collection and preservation of cells, 2) flow cytometric sorting of specific phytoplankton groups, heterotrophic bacteria, and non-living organic matter (detritus) from bulk PN collections, 3) conversion of sorted organic PN to nitrate by persulfate oxidation, 4) quantitative bacterial conversion of nitrate to nitrous oxide, and subsequent measurement of the isotopic composition of the nitrous oxide. Steps 1 and 2 are described below in detail. For steps 3 and 4, we focus on the specifics related to the sample type analyzed here; general application of these steps are described in [50,51].

1.1. Sample collection

Samples were collected aboard the R/V *Atlantic Explorer* at Hydrostation S (32°10' N, 64°34' W) on cruise HS1113 in July 2008 and at PITS station (31°35' N, 64°10' W) on Bermuda Atlantic Time-series Study (BATS) cruise B248 in July 2009. Seawater was collected for PN and nitrate (NO_3^-) at various depths through the euphotic zone, based on CTD hydrogrographic and fluorescence data from previous casts on that cruise: surface, 10 m, 40 m, 85 m and 100 m in 2008; and 10 m, 30 m, 60 m, and 100 m in 2009. The deep chlorophyll maximum (DCM) was located at 85 m in 2008 and 100 m in 2009 (causing us to sample at these depths), and the mixed layer depth (MLD) was ~20 m in both years. Five 12 L Niskin bottles were tripped at each depth in order to collect sufficient PN for later isotope analysis. In addition, Niskin bottles were tripped at regular intervals from below the euphotic zone down to 1000 m (see figs. 2A-D and S6A-D for PN sample depths, and fig. 1 for NO_3^- sample depths). 500 mL (shallow) and 60 mL (deep) seawater samples were sub-sampled from each Niskin bottle and immediately frozen at -20°C for later measurement of nitrate concentration ($[NO_3^-]$) and nitrate $\delta^{15}N$.

The remaining seawater in the shallower Niskin bottles was transferred into acid-washed 4 L Thermo Scientific Nalgene LDPE carboys with attached ¼ inch acid-cleaned tygon tubing. The tubing was attached to 47 mm acid-washed inline polycarbonate filter holders containing 0.4 μm polycarbonate filters. 8 L of seawater was passed through each filter under gentle vacuum filtration (<100 mm Hg). Filtration was stopped before filters went dry, and filters were removed from the holders and transferred to acid-washed 5 mL cryovials. Approximately 4 mL of pre-filtered (0.2 μm polycarbonate filter) seawater was added to the cryovials along with 200 μL of 10% formaldehyde solution (PFA; ~0.5% final concentration; see below for discussion of PFA use). Cryovials were agitated to dislodge cells from the filter and encourage 'fixation' by the PFA. Samples were incubated at 4°C for 1-2 hours and then flash-frozen in liquid nitrogen. After the cruise, cryovials were transferred from the liquid nitrogen to a -80°C freezer, where they were stored for later flow cytometric sorting.

In July 2008, 8 L aliquots of seawater taken from 20 m depth increments from the surface down to 100 m were filtered onto precombusted glass fiber filters (GF/Fs) to capture bulk PN. The total N content and $\delta^{15}N$ of these samples was analyzed using an elemental analyzer (NC2500 Carlo Erba) coupled with a ConFlo III interface on a ThermoFischer Scientific DeltaPlusXL mass spectrometer at the GeoForschungsZentrum in Potsdam. In

July 2009, bulk PN was filtered from 8 L seawater aliquots collected from 10 m, 30 m, 60 m and 100 m onto 0.4 μm polycarbonate filters and processed in the same manner as PN samples collected for flow cytometry.

1.2. Laboratory methods

1.2.1. Sample preparation for flow cytometric sorting and analysis

Samples in cryovials were thawed at room temperature in the dark and agitated to remove as many fixed cells as possible from the filters. Used filters were later measured for remaining N content, which was found to be negligible. Cells in solution were then filtered through a 30 μm mesh in order to remove the occasional large heterotrophic particle, and any chains of cells that could clog the sorting tip of the flow cytometer. If necessary, samples were diluted with 0.2 μm-filtered seawater so as to attain an appropriate cell concentration for flow cytometric sorting. All samples were sorted at Bermuda Institute of Ocean Sciences in the laboratory of Dr. Michael Lomas.

1.2.2. Gating

Samples were analyzed or sorted for the picocyanobacteria *Prochlorococcus* and *Synechococccus*, two size classes of eukaryotic algae, heterotrophic bacteria, and "detritus". Autotrophs were identified and sorted unstained according to gating schema described elsewhere[52] (see fig. S1 for an example cytogram). After exclusion of laser noise gated on forward scatter pulse height (FSC-H) and pulse width, autotrophic cells were identified by red (650nm LP) autofluoresescence, which is roughly indicative of chlorophyll content. Among the picocyanobacteria, *Synechococcus* was discriminated from *Prochlorococcus* by FSC-H and the yellow/orange (580/30nm) fluorescence of phycoerythrin. Autotrophs not included in the cyanobacteria gates were assumed to be eukaryotic algae. Gating for two eukaryotic algae size fractions ("picoeukaryotes" and "nanoeukaryotes") was delineated by the peak FSC-H channel from a histogram created before sorting using 3.0 μm polystyrene calibration particles (Spherotech, Inc., Lake Forest, IL). Ultimately however, in order to ensure sufficient N mass for isotope analysis, "picoeukaryotes" and "nanoeukaryotes" sorted from the same PN collection were combined and considered "total eukaryotes". A pool of heterotrophic bacteria (likely including some archaea, but hereafter simply "bacteria") were identified by nucleic acid staining with the cyanine dye SYTO-13 (Invitrogen Co., Carlsbad, CA) and gated with side scatter, green fluorescence (relative nucleic acid content; 530/40nm), and red fluorescence to discriminate low nucleic acid content heterotrophic bacteria from *Prochlorococcus* (adapted from [53]). "Detritus" was defined as non-fluorescing small particles (<3.0 μm polystyrene bead forward scatter equivalent) in SYTO-13 stained samples. In some cases, boolean gating was used for sorting "total cyanobacteria" or "total eukaryotes". All post acquisition analysis was performed using FCS Express (DeNovo Software, Los Angeles, CA).

1.2.3. Sort conditions

A high speed jet-in-air Influx Cell Sorter (Cytopeia, Inc., Seattle, WA) was used for all analysis and sorts. A 100 mW blue (488nm) laser (Coherent Inc., Santa Clara, CA) run at full power was used for excitation of SYTO-13 stained and autofluorescent cells. Analog pulse height signals from 530/20nm, 580/30nm, 650LP, side scatter (SSC), and FSC

photomultiplier tubes (Hamamatsu Photonics K.K.) were log amplified and converted to 16 bit listmode data in the FCS3.0 format using the acquisition software Spigot V.6.1.4 (Cytopeia Inc., Seattle, WA). Detector and jet alignment was optimized using 0.53 μm Nile Red polystyrene calibration particles (Spherotech Inc., Lake Forest, IL). A 70 μm ceramic nozzle tip was used with a sample pressure of 28.5 Psi (+1.0 Psi above sheath pressure) to optimize speed while maintaining high fluorescent yield and ensuring laminar flow. A square waveform at 988KHz master clock frequency was applied to the nozzle tip producing a droplet formation frequency of 61.75KHz. The sample flow rate at this configuration was roughly 40 μL min^{-1}. Sheath fluid was made fresh daily from 0.22 μm filtered distilled deionized Milli-Q water (Millipore Inc., Billerica, MA) and molecular grade NaCl (Mallinckrodt Baker Inc., Phillipsburg, NJ), and filter sterilized in-line through a 0.22 μm Millifil capsule filter (Millipore Inc., Billerica, MA). Where necessary, coincident event detection of ±1 droplet was used to improve sort purity. To minimize software abort rates at the described droplet formation rate and coincident detection settings, event rates were maintained below 20,000 s^{-1}. Although decompression injury to cell membrane integrity is of concern to intracellular staining of live mammalian cells[54,55], cells such as those investigated in this study experience pressure changes during sample collection more than an order of magnitude higher than those experienced during the sorting process (ca. 18 dBar at our sort configuration).

With the sort configurations outlined above, software abort rates were <1%. Regular analysis of sorted populations demonstrated that sort purity was better than 95% (calculated as the proportion of sorted events which fell into the prescribed gating schema as a percentage of total event rate), and mean recovery from sorts was 98.1±1.1% (calculated as the number of target events recovered as a percentage of the number of positive sort decisions recorded by the acquisition software). It should be noted that any sort contamination would have been comprised mainly of particles at or near the forward scatter detection limit, i.e., predominantly very tiny non-cellular particles. Thus, even at ca. 5% contamination by particle count, the N mass contributed by any contaminant particles would be minute and would not affect the measured N isotope values. Cells were deposited gently into 5 mL polystyrene Falcon tubes (BD Biosciences Inc., San Jose, CA) by orienting the side-wall of the tube nearly parallel to the sort stream.

With limited *a priori* knowledge of cellular PN quotas, we conservatively anticipated the number of cells needed to exceed twice the minimum mass required for downstream analysis by converting known particulate organic carbon cellular quotas to nitrogen by the Redfield stoichiometric coefficient. Thus, sorts were typically terminated once the volume available was exhausted. Since sufficient yield often required sort times of one to three hours per population (depending on relative natural abundances), care was taken to ensure minimal exposure to room temperatures by immediately refrigerating portions of the sort.

1.2.4. Persulfate oxidation of organic N to NO_3^-

Sorted cell populations in Falcon tubes were filtered onto 25 mm 0.2 μm polycarbonate filters by gentle vacuum filtration, and washed with copious amount of 0.2 μm filter-sterilized low nutrient Sargasso Seawater. Both sorted and bulk PN sample filters were

placed in combusted 12 mL Wheaton vials and 1 mL and 2 mL of ultra-high purity deionized water (DIW) was added to the sorted samples and bulk PN samples, respectively. Vials were sonicated for 60 minutes to remove cells from the filters and suspend them in the DIW, after which the filters were removed. Used filters were later measured for remaining N content, which was found to be negligible.

The organic N suspended in DIW in the vials was then oxidized to nitrate according to the persulfate oxidation method of [50]. Briefly, 0.5 mL of potassium persulfate oxidizing reagent (POR) was added to sorted samples, and 1 mL to bulk samples and triplicate samples of two amino acid standards (glycine and aminocaproic acid). The POR was made from 6 g sodium hydroxide and 6 g of four-times recrystallized potassium persulfate in 100 mL of DIW. The procedure used for persulfate recrystallization is described in [56]. Sample vials were capped tightly after the addition of the POR, weighed, and autoclaved at 121˚ C for 55 minutes on a slow-vent setting, before being weighed again to ensure no loss or gain to the vials. Three vials of POR, and six vials of DIW + POR were also autoclaved to determine the N blank associated with the POR.

After oxidation of the samples to nitrate, the pH in the vials was lowered to between 5 and 9 using 12N HCl, in order to prevent the high pH of the POR killing the denitrifying bacteria. After pH adjustment, the concentration and $\delta^{15}N$ of the resultant NO_3^- was measured using chemiluminescent analysis and the "denitrifier method"[57-59], allowing analysis of flow cytometrically-sorted fractions containing as little as 10 nmol N. The final N content and $\delta^{15}N$ of these oxidized samples was corrected for the N blank associated with the POR. N content was converted to N concentration ([N]) using the seawater volume filtered for each PN sample, corrected for volume loss during flow cytometry (both to waste and dilution). Error is reported for replicate samples, and not for replicate measurements of the same sample, in order to characterize the precision of the full protocol.

1.2.5. Water column nitrate concentration and $\delta^{15}N$

Water samples were collected for $[NO_3^-]$ from the surface to 1000 m, and for $\delta^{15}N\text{-}NO_3^-$ from 60 m to 1000 m at the two stations (Hydrostation S in 2008 and PITS in 2009). $[NO_3^-]$ was determined by injecting 100 – 250 μL of seawater sample into a 90°C acidic solution of vanadium (V(III))[59,60], in a configuration with a detection limit of ~0.025 μM. This measurement nominally includes nitrite, but nitrite concentrations were negligible relative to nitrate in all samples. The vanadium solution reduces NO_3^- to nitric oxide gas, which reacts with ozone, releasing photons that are detected by a photomultiplier inside a chemiluminescent detector (Teledyne model #200 EU).

The $\delta^{15}N$ of NO_3^- was measured using the "denitrifier method", which involves quantitative bacterial conversion of nitrate to nitrous oxide[57] for samples. The isotopic composition of the nitrous oxide was measured by gas chromatography-isotope ratio mass spectrometry using a modified ThermoFinnigan GasBench II and DeltaPlus[58]. Nitrate $\delta^{15}N$ measurements are reported as average values ± 1 standard error, as multiple samples were taken from each depth, and each sample was analyzed at least three times. Where error bars are not visible, they are smaller than the data markers.

2. Methods validation data

Phytoplankton cells must be "fixed" in order to be sorted by flow cytometry. Because cells are sorted on the basis of light scatter and natural fluorescence, the fixation procedure must preserve these characteristics. A formaldehyde solution (PFA, made by heating paraformaldehyde powder in DIW) is commonly used for fixation because it minimizes cell disruption and does not strongly modify the pH of seawater samples[69]. PFA is a cross-linking fixative that creates covalent chemical bonds between proteins in tissue. It allows for long-term storage of "fixed" cells as well as later penetration of DNA stains such as SYTO-13 through the cell membrane (*see SI 1.2.2*).

Formaldehyde is known to alter the $\delta^{13}C$ of preserved samples and may have an effect on $\delta^{15}N$ under some conditions ([61] and refs therein). In order to ensure that our methodological approach did not alter the $\delta^{15}N$ of sorted PN samples, we conducted a series of experiments: Triplicate cultures of the marine diatom *Thalassiosira weissflogii* were grown with 40 μM amendment of the nitrate reference material IAEA N3 ($\delta^{15}N$ = 4.7‰[62]). Cells were harvested once nitrate had been completely consumed, at which stage the $\delta^{15}N$ of cellular organic N is expected to converge on the $\delta^{15}N$ of the nitrate supply. Six subsamples (duplicates for each of three treatments) of each *T. weisfloggi* culture were filtered onto 5 μm polycarbonate filters by gentle vacuum filtration. One set of duplicates was flash frozen without any manipulation ("without PFA"; fig. S2), and PFA + 0.2 μm filtered seawater was added to the remaining two sets of duplicates. One set of these samples was then run through the flow cytometer ("FACS sorted"; fig. S2), and the remaining fixed set was not sorted ("with PFA"; fig. S2). All samples were then processed in the same way as the PN collections described above. The results indicate that neither fixation by PFA nor FACS sorting significantly altered the $\delta^{15}N$ of cellular organic N (fig. S2).

3. Supplemental notes and discussion

3.1. Different N uptake capabilities of the Sargasso Sea phytoplankton assemblage
Culture studies have shown that all ecotypes of *Prochlorococcus* grow well on NH_4^+ and urea, and some low-light strains can grow on NO_2^-[63,64]. High *in situ* rates of organic N assimilation by *Prochloroccocus* have been reported for the Arabian Sea and the South Atlantic subtropical front[65,66]. To date, no cultured ecotypes of *Prochlorococcus* have displayed uptake of nitrate, although natural *Prochlorococcus* populations in the Sargasso Sea have been shown to possess nitrate assimilation genes[67] and ^{15}N incubations suggest that they may acquire 5-10 % of their N from NO_3^-[68]. Cultured marine *Synechococcus* spp. have been reported to utilize NH_4^+, NO_2^-, NO_3^-, urea, and amino acids[64,69-73], and under severe N deprivation will even degrade their own light-harvesting pigment protein, phycoerythrin, to use as an internal N source[74]. It is well known that eukaryotic phytoplankton can utilize all forms of fixed N, as well as urea and amino acids ([75] and refs therein). However, it is generally accepted that in the nutrient poor subtropical ocean, NH_4^+ is the dominant N source supporting all phytoplankton growth, including that of the eukaryotic phytoplankton[76-78].

3.2. Alternate explanations for high eukaryote $\delta^{15}N$
One set of hypotheses for the high eukaryote $\delta^{15}N$ is control by some mechanism of N loss, such as the excretion of NO_2^- or NH_4^+. Another involves the assimilation of NO_3^- generated by nitrification in the euphotic zone. The hypotheses are discussed below.

3.2.1 Nitrite efflux
It has been suggested to us that the $\delta^{15}N$ of eukaryote biomass could be elevated beyond the $\delta^{15}N$ of the nitrate supply if low $\delta^{15}N$ nitrite is excreted from the cell during nitrate assimilation. Nitrite efflux seems exceedingly unlikely, as it requires that phytoplankton excrete nitrite throughout the water column in an extremely N-deplete euphotic zone. However, whether or not nitrite efflux occurs does not actually matter, because the isotope systematics of nitrate assimilation are such that nitrite efflux does not provide an explanation for the data (fig. S3 and S4A-B).

During assimilation, nitrate is transported across the cell membrane with minimal isotopic fractionation (ε_1, ε_2 = 0‰; fig S3), and is then reduced in the cytoplasm to nitrite by the nitrate reductase enzyme. Nitrate reductase has an isotope effect (ε_3; fig S3) of ~25‰ (e.g., [79]). For a common case of ~80% reduction for the gross nitrate uptake[80], the internal nitrate pool comes to have a $\delta^{15}N$ of 20‰ and the produced nitrite has a $\delta^{15}N$ of -5‰. This nitrite is transported into the chloroplast (with ε_4 = 0‰; fig S3) where it is completely reduced to NH_4^+ and then converted into organic N (represented by the thick black arrow between NO_2^- and Org N). The nitrite imported into the chloroplast is efficiently and completely reduced, and thus there is no isotopic fractionation associated with either reduction step[79,81]). The organic N (biomass) that is produced has a $\delta^{15}N$ = -5‰.

If nitrite efflux were to occur, the nitrite excreted from the cell has the same $\delta^{15}N$ as the nitrite taken up into the chloroplast (-5‰), since it is implausible that efflux of nitrite

from the cell could have a higher isotope effect than nitrite uptake by the chloroplast (ε_4, ε_5 = 0‰; fig S3). As a result, the biomass produced has a $\delta^{15}N$ of -5‰ regardless of the fraction of the nitrite pool that effluxes from the chloroplast. While it is possible that ε_4 could be ~1-2‰ higher than ε_5, this would cause nitrite efflux to lower, not raise, the $\delta^{15}N$ of the biomass produced.

Having established that the excretion of nitrite cannot increase the $\delta^{15}N$ of eukaryotic phytoplankton beyond the $\delta^{15}N$ of the nitrate they are assimilating, there are two additional relevant points to be made with respect to nitrite efflux:

First, in order for nitrite efflux to occur, the eukaryotes need to be assimilating nitrate. Since the cyanobacteria are not elevated in $\delta^{15}N$, they must not be consuming nitrate. Thus, even if nitrite efflux is important, our major conclusion that eukaryotic phytoplankton dominate the consumption of nitrate in the subtropical euphotic zone still holds.

Second, cultures do not excrete nitrite during balanced growth. Most of the studies that report nitrite efflux during nitrate assimilation involve cultures at stationary phase (see review by [81]), meaning that the phytoplankton cells have run out of nutrients and become senescent. These cultures are not representative of the phytoplankton community we sampled, and offer no reason to expect persistent and substantial nitrite efflux from eukaryotic phytoplankton throughout the summertime euphotic zone of the Sargasso Sea.

When observed, nitrite excretion is a transient process. Efflux has been observed in response to transient light limitation (e.g., [82], wherein phytoplankton mixed down below the 1% light level can no longer harness the reducing power required to convert intracellular nitrite to ammonium; rather than allow nitrite to accumulate inside the cell, they excrete it. This behaviour speaks to the toxicity of nitrite to cells[83-85], and represents a transient, rather than a steady state nitrite efflux. One study found that even under conditions of light limitation, the assimilation of nitrate by diatoms in steady state growth was limited by the reduction of nitrate to nitrite[86], arguing against any intracellular nitrite accumulation, and thus any possibility of continuous nitrite efflux.

As one exception to this, nitrite excretion by cells during balanced growth has been observed in a limited number of studies under iron limitation. It has been hypothesized that under such low iron conditions nitrite reduction may become the limiting step in nitrate assimilation due to the high Fe requirement of nitrite reductase (NiR)[87,88]. Under this condition, nitrite could be excreted into the environment in order to alleviate intracellular toxicity[83-85]. However, iron limitation of phytoplankton is unlikely in the Sargasso Sea euphotic zone[89-91], particularly in the summer when atmospheric dust inputs of iron are high[92]. Thus, while it is possible that phytoplankton may excrete nitrite under certain conditions, physiological constraints such as enzyme affinity for substrate as well as euphotic zone conditions in the Sargasso Sea at the time of our sampling render such efflux unlikely.

3.2.2. Mixotrophy and associated ammonium efflux

Given the well-known increase in biomass $\delta^{15}N$ with trophic level[93,94], the high eukaryotic $\delta^{15}N$ might be intuitively attributed to some degree of heterotrophy ("mixotrophy"). Mixotrophy by small eukaryotic phytoplankton has been suggested as significant in both the western and eastern North Atlantic[95-97], although the abundance of mixotrophs is generally low and highly variable, both with depth and time of sampling. In any case, it must be recalled that the trophic $\delta^{15}N$ increase derives from the excretion by heterotrophs of low-$\delta^{15}N$ N[93,98]. In the nutrient-poor summertime Sargasso Sea, it is unlikely that phytoplankton will excrete NH_4^+, and yet eukaryotes would need to excrete nearly all the N they obtain from heterotrophy in order to achieve a ≥3‰ $\delta^{15}N$ elevation relative to prokaryotes (given that this amplitude of $\delta^{15}N$ increase corresponds to a single trophic level in heterotrophs[99]).

Our 2009 eukaryote sample from the mixed layer, the depth at which mixotrophy has been suggested to be most likely, has the lowest $\delta^{15}N$ of all measured eukaryote samples. We interpret this to reflect increased reliance by surface eukaryotes on recycled N in response to being isolated from the deep nitrate supply. If mixotrophy is responsible for high eukaryote $\delta^{15}N$, and mixotrophy is most likely to occur in the summertime mixed layer, we would expect the surface eukaryote sample from 2009 to be higher in $\delta^{15}N$. This is not what we observe.

A key additional observation from our study is that a sorted population of heterotrophic bacteria has a $\delta^{15}N$ similar to that of the cyanobacteria (-1.0‰; fig. 2B and S6B). These heterotrophic bacteria are far more likely to excrete ammonium than are the eukaryotic phytoplankton as they are not photosynthesizing, yet their $\delta^{15}N$ is not elevated relative to the cyanobacteria. In order for mixotrophy to be responsible for the high eukaryote $\delta^{15}N$, high levels of N excretion are required. The lack of isotopic elevation in heterotrophic bacteria provides another strong piece of evidence against mixotrophy as the driver of the high $\delta^{15}N$ of the eukaryotes. Thus, while it is always possible that some as yet unidentified process is responsible for the high $\delta^{15}N$ of the eukaryotes, no clear loss-based explanations have been recognized.

3.2.3. Nitrification

We conclude that the high eukaryote $\delta^{15}N$ must derive from the assimilation of a high-$\delta^{15}N$ N source, most likely nitrate. Nitrate could be supplied by *in situ* nitrification (oxidation of recycled NH_4^+ to nitrite and then nitrate) or by upward mixing of subsurface nitrate. Nitrification is usually found to be negligible in the subtropical euphotic zone[82], although some fraction of the very low-level summertime ambient nitrate at BATS may derive from nitrification[100].

Regenerated NH_4^+ can either be re-assimilated by phytoplankton or oxidized to NO_2^-, which will then either be assimilated into PN or further oxidized to NO_3^-. The relative size of the isotope effects associated with each of these processes will affect the $\delta^{15}N$ of both the PN and NO_3^- pools. If the combined isotope effect associated with NH_4^+ and NO_2^- assimilation (ε_{AmU} and ε_{NiU}, respectively, after [101]) is larger than that due to nitrification (ε_{Nitr}, reflecting the combined fractionation associated with NH_4^+ oxidation

and NO_2^- oxidation, ε_{AmOx} and ε_{NiOx}, respectively, after [101]), high-$\delta^{15}N$ N will be preferentially channeled into the NO_3^- pool, implying that some portion of the eukaryotes' high-$\delta^{15}N$ NO_3^- supply could derive from a regenerated N source.

Culture studies report ε_{AmU} as high as 27 ‰, but this value decreases to 0 – 1 ‰ at low $[NH_4^+]$[102-104], likely due to very low rates of NH_4^+ efflux preventing expression outside the cell of any fractionation associated with intracellular NH_4^+-consuming reactions. In the Sargasso Sea, NH_4^+ concentrations are always extremely low[100], such that the expressed ε_{AmU} will approach ~0 ‰. ε_{NiU} is thought to be similarly low[105].

Cultured marine nitrifiers yield values of ε_{AmOx} from 14 ‰ to 19 ‰[106,107]. It is unlikely that ε_{AmOx} decreases much at low $[NH_4^+]$ because fractionation occurs in the periplasm of nitrifying bacteria (Hooper et al. 1997) where ε_{AmOx} is less vulnerable to under-expression by NH_4^+ consumption within the cell[108]. Additionally, the ammonium/ ammonia equilibrium isotope effect (~20 ‰[109,110]) included in ε_{AmOx} does not decrease at low $[NH_4^+]$. Nitrite oxidation has an 'inverse' isotope effect (ε_{NiOx} ~ -12 ‰[111], but the nitrite oxidoreductase enzyme is located in the cytoplasm of nitrite oxidizing bacteria[112], and is thus subject to under-expression at low substrate concentrations. Since NO_2^- does not accumulate above nanomolar concentrations in the Sargasso Sea[113], the expressed value of ε_{NiOx} will be ~0 ‰. Thus, we consider only isotope fractionations associated with NH_4^+ reactions. At the low $[NH_4^+]$ typical of the Sargasso Sea, $\varepsilon_{AmOx} - \varepsilon_{AmU}$ (and thus $\varepsilon_{Nitr} - \varepsilon_{AmU}$) > 0 ‰, and any nitrification will channel low-$\delta^{15}N$ N into the NO_3^- pool. Therefore, our high $\delta^{15}N$ eukaryote measurements are unlikely to reflect assimilation of NO_3^- regenerated within the euphotic zone: even if euphotic zone nitrification were significant, the assimilation of its products by eukaryotes does not explain their clear $\delta^{15}N$ elevation relative to prokaryotes.

3.3. $\delta^{15}N$ relationship between nitrate supply and phytoplankton biomass
See figure S5 and figure S5 caption.

3.4. Mechanism controlling N source differences
While we do not understand the mechanism controlling N source differences, there are potential explanations. Given that it is less energetically expensive to assimilate reduced N forms[114], the rapidly cycling N pool should be most prized. Thus, rather than eukaryotes outcompeting prokaryotes for nitrate, prokaryotic phytoplankton may be outcompeting eukaryotes for recycled N. In this view, eukaryotes have secured their position in the ecosystem partly by populating the niche of consuming an energetically expensive N source.

Alternatively, eukaryotes may indeed be better at utilizing nitrate, with the key to eukaryotic exploitation of very low nitrate concentrations being the uncoupling of nitrate transport from nitrate reduction. Both eukaryotes and prokaryotes possess high affinity nitrate transporters, encoded by *Nrt2* genes. Eukaryotes typically have multiple *Nrt2* gene copies per genome[115], indicative of an activity that can be rapidly induced and highly modulated. Cyanobacterial genomes usually contain only one *Nrt2* gene[116], and transport is tightly coupled to photosynthesis[117]. Thus, the eukaryote advantage might be in their ability to respond to episodic nitrate availability by rapidly transporting nitrate into the

cell, where the slower step of nitrate reduction can occur[118], removed from competition with prokaryotes.

3.5. Calculation of the f-ratio

The f-ratio is traditionally defined as the ratio of new production (i.e., supported by thermocline nitrate) to total primary production (the sum of new plus regenerated production, the latter of which is supported by NH_4^+, simple organic N forms, and nitrite and nitrate produced by *in situ* nitrification). The f-ratio also quantifies the fraction of primary production that is exported from the euphotic zone over appropriate time and space scales (i.e., export production)[76,119]. At BATS, total primary production is routinely measured by ^{14}C uptake in dawn to dusk *in situ* incubations[78]. From 1989 to 1997, the mean value of total primary production, integrated from 0-140 m, was 154.2±28.9 gC m^{-2} yr^{-1}. The sediment trap flux at 150 m, averaged over the same time period, was 9.4±1.4 gC m^{-2} yr^{-1}, which, when divided by total primary production, implies an export ratio (f-ratio) of 0.06±0.01[78].

In the current study, the f-ratio for July of each year (2008 and 2009) is estimated according to the following equations:

$$f_{community} = \{f_{Pro}*[N]_{Pro} + f_{Syn}*[N]_{Syn} + f_{euk}*[N]_{euk}\}/\{[N]_{Pro} + [N]_{Syn} + [N]_{euk} \quad (1)$$

where: $\delta^{15}N_{Pro} = \delta^{15}N_{NN}*f_{Pro} + \delta^{15}N_{RN}*(1-f_{Pro})$

such that $f_{Pro} = (\delta^{15}N_{Pro} - \delta^{15}N_{RN})/(\delta^{15}N_{NN} - \delta^{15}N_{RN})$ (2)

$$\delta^{15}N_{Syn} = \delta^{15}N_{NN}*f_{Syn} + \delta^{15}N_{RN}*(1-f_{Syn})$$

such that $f_{Syn} = (\delta^{15}N_{Syn} - \delta^{15}N_{RN})/(\delta^{15}N_{NN} - \delta^{15}N_{RN})$ (3)

$$\delta^{15}N_{euk} = \delta^{15}N_{NN}*f_{euk} + \delta^{15}N_{RN}*(1-f_{euk})$$

such that $f_{euk} = (\delta^{15}N_{euk} - \delta^{15}N_{RN})/(\delta^{15}N_{NN} - \delta^{15}N_{RN})$ (4)

The $\delta^{15}N$ used in the formulation above for each sorted population (i.e., $\delta^{15}N_{Pro}$, $\delta^{15}N_{Syn}$, and $\delta^{15}N_{euk}$) is the N concentration-weighted mean $\delta^{15}N$ of that population integrated over the euphotic zone. This formulation assumes that all groups have the same specific growth rate, although other assumptions, such as a higher growth rate for eukaryotes, could be used. More importantly, this exercise is highly dependent on the $\delta^{15}N$ assigned to NN (new N) and RN (regenerated N; including NH_4^+, simple organic N forms, and nitrite and nitrate produced by euphotic zone nitrification). We have no direct information on the $\delta^{15}N$ of the RN supply, but if we assume that *Prochlorococcus* and *Synechococcus* together assimilate only RN, then water column integrated prokaryote $\delta^{15}N$ (0 – 100 m) yields a $\delta^{15}N$-RN of -1.2 ‰ in 2008 and -1.9 ‰ in 2009. For $\delta^{15}N$-NN, we use the $\delta^{15}N$ of nitrate at the DCM (6.2‰ in 2008 and 8.4‰ in 2009 (fig.1B) at depths of 85 m and 100 m, and $[NO_3^-]$ of 0.49 μM and 0.36 μM, respectively) as our best

measure of the nitrate supply to the euphotic zone in July. N_2 fixation is a potential additional source of NN to the system; however, since its $\delta^{15}N$ is low (-2 to 0‰)[120], our exclusion of this term translates to an underestimation of the f-ratio. Finally, we assume that our collected eukaryote samples are randomly distributed with regard to the degree that the new nitrate supply had been consumed when they were assimilating it. In this case, with or without isotope fractionation during assimilation, the mean $\delta^{15}N$ of discrete samples of phytoplankton assimilating only nitrate should approximate the $\delta^{15}N$ of the initial nitrate supply (*see SI 3.3*). Among the uncertainties mentioned above, we highlight the $\delta^{15}N$ of the nitrate supply; if some nitrate is imported from significantly deeper than the DCM[121], then $\delta^{15}N$-NN would be lower than assumed, yielding an even higher f-ratio for the eukaryotes. This only further reinforces our interpretation that nitrate transported into the euphotic zone from below supports more than half of the summertime eukaryote productivity, corroborating the proposed importance of such processes as eddy-induced upwelling[121,122].

A number of studies have used geochemical measures such as O_2 production in the euphotic zone, O_2 utilization in the thermocline, and long-term changes in the thermocline inventory of $^3H + {}^3He$ to estimate the upward flux of nitrate from the thermocline into the Sargasso Sea euphotic zone[123-126]. This nitrate flux can be considered an estimate of new production, and on an annual basis, will be balanced by the export of PN + DON from the euphotic zone to the deep ocean. Using geochemically derived nitrate fluxes (Table S1), and converting total primary production as reported above to mol N m^{-2} yr^{-1} by assuming Redfield stoichiometry[127], we can estimate the f-ratio implied by the geochemical tracers (0.20±0.09 to 0.36±0.12; Table S1).

Nitrate flux (mol N m^{-2} yr^{-1})	Geochemical method	Implied f-ratio	Reference
0.42±0.09	O_2 utilization	0.22±0.06	123
0.46±0.09	O_2 production	0.24±0.06	123
0.56±0.16	Tritium + ^{3}He flux	0.29±0.10	126
0.39±0.16	O_2 production	0.20±0.09	124
0.51±0.14	O_2 production	0.26±0.09	124
0.70±0.20	Tritium + ^{3}He flux	0.36±0.12	125

Table S1: Estimates of the annually integrated f-ratio at BATS using geochemically derived nitrate fluxes (mean ± 1 SD) as a measure of new production, and the average ^{14}C uptake-based measurement of total primary production (1.94±0.36 mol N m^{-2} yr^{-1} as described above)[78].

3.6. Contribution of eukaryotic phytoplankton to the sinking flux PN

Using the measured [N] and $\delta^{15}N$ of our sorted populations, we can estimate the contribution of eukaryotic phytoplankton to the sinking flux. We calculate the $\delta^{15}N$ of the non-eukaryotic PN ($\delta^{15}N_{non\text{-}euk}$), which includes prokaryotic PN (*Prochlorococcus* + *Synechococcus*; $\delta^{15}N_{prok}$) and the unmeasured component of the PN ($\delta^{15}N_{unmeas}$, as described above), and for 2008 also includes the detrital PN ($\delta^{15}N_{det}$) and heterotrophic bacterial PN ($\delta^{15}N_{hb}$).

For 2008:

$$\delta^{15}N_{non\text{-}euk} = ((\delta^{15}N_{prok}*[N]_{prok}) + (\delta^{15}N_{unmeas}*[N]_{unmeas}) + (\delta^{15}N_{det}*[N]_{det}) + (\delta^{15}N_{hb}*[N]_{hb}))/ ([N]_{prok} + [N]_{unmeas} + [N]_{det} + [N]_{hb}) \quad (5)$$

For 2009:

$$\delta^{15}N_{non\text{-}euk} = ((\delta^{15}N_{prok}*[N]_{prok}) + (\delta^{15}N_{unmeas}*[N]_{unmeas}))/([N]_{prok} + [N]_{unmeas}) \quad (6)$$

where: $\delta^{15}N_{prok} = ((\delta^{15}N_{Pro}*[N]_{Pro}) + (\delta^{15}N_{Syn}*[N]_{Syn}))/([N]_{Pro} + [N]_{Syn})$ (7)

All $\delta^{15}N$ values used in the formulation above, and reported in Table S2, are the N concentration-weighted mean $\delta^{15}N$ for each sorted population, integrated over all measurements in the water column. By combining the measurements from the two years, N concentration-weighted "summertime average" $\delta^{15}N$ values are calculated.

The flux of sinking organic matter from the euphotic zone is likely comprised predominantly of PN that has been repackaged by herbivorous zooplankton as fecal pellets, rather than individual phytoplankton or heterotrophic cells. There is some debate as to the isotope discrimination associated with the generation of these fecal pellets, with some studies suggesting that they are isotopically similar to zooplankton biomass (i.e., elevated by ≥ 2‰ relative to the zooplankton food source[128,129] and others reporting fecal pellet $\delta^{15}N$ values similar to the consumed material[130,131]. For the purpose of this demonstrative exercise, we take fecal pellet $\delta^{15}N$ to be 1‰ higher than the $\delta^{15}N$ of the various sorted populations, such that the "summertime average" eukaryotic component of the sinking flux ($\delta^{15}N_{fp\text{-}euk}$) becomes 5.1‰, and the non-eukaryotic component ($\delta^{15}N_{fp\text{-}non\text{-}euk}$) increases to -0.5‰ (Table S2).

Table S2

Water column integrated $\delta^{15}N$	**July 2008 (‰)**	**July 2009 (‰)**	**"Summertime average" (‰)**
$\delta^{15}N_{euk}$	3.0	5.0	4.1
$\delta^{15}N_{prok}$	-1.2	-1.9	-1.5
$\delta^{15}N_{det}$	-0.3	ND	-0.3
$\delta^{15}N_{hb}$	-1.0	ND	-1.0
$\delta^{15}N_{unmeas}$	-1.1	-1.6	-1.3
$\delta^{15}N_{non\text{-}euk}$	-1.0	-1.7	-1.3
$\delta^{15}N_{fp\text{-}euk}$	**4.0**	**6.0**	**5.1**
$\delta^{15}N_{fp\text{-}non\text{-}euk}$	**-0.2**	**-0.9**	**-0.5**

Previous measurements of the $\delta^{15}N$ of the sinking flux ($\delta^{15}N_{sink}$) from material caught in sediment traps at 150 m at the BATS site range from 3-4‰[132]. It should be noted that this value of $\delta^{15}N_{sink}$ is based on a single study consisting of near-monthly particle collections over the course of two years (1985-1986)[132]. Using the $\delta^{15}N_{fp\text{-}euk}$ and $\delta^{15}N_{fp\text{-}non\text{-}euk}$ values from Table S2, and $\delta^{15}N_{sink}$ = 3.5‰, we calculate a potential "summertime average" eukaryotic contribution to the export flux of 71% according to:

Euk contribution (%) = $\{(\delta^{15}N_{sink} - \delta^{15}N_{fp\text{-}non\text{-}euk})/(\delta^{15}N_{fp\text{-}euk} - \delta^{15}N_{fp\text{-}non\text{-}euk})\}*100$ (8)

We acknowledge that there is likely some contribution to $\delta^{15}N_{sink}$ of unconsumed material, passively sinking out of the surface ocean as aggregates or marine snow[133,134]. If included, this unfractionated material would likely only serve to increase the calculated eukaryotic contribution to the sinking flux, further strengthening our conclusion that eukaryotic phytoplankton are the dominant contributors to sinking PN.

3.7. [N] and $\delta^{15}N$ of "sum" and "missing" N pools

For both 2008 and 2009, we calculate the summed N content ([N]) of the sorted populations ("sum") by adding $[N]_{Pro}$, $[N]_{Syn}$ (or $[N]_{Total\text{-}cyano}$) and $[N]_{euk}$ (and $[N]_{hetero\text{-}bacteria}$ or $[N]_{detritus}$ in the case of the surface and 40 m samples from 2008; fig. S6A and C). In cases where we do not have measurements of all photoautotrophic N pools, we still add the [N] measurements that we do have to get a $[N]_{sum}$, but do not include these values in further calculations of the contribution of photoautotrophic N to total PN (i.e., photoautotrophic contribution (%) = $([N]_{sum}/[N]_{bulk})*100$). For both years, <50% of the bulk PN in the Sargasso Sea appears to be comprised of photoautotrophic N, as demonstrated by the summed N value of all our sorted populations (fig. S6A and C), and in agreement with previous studies of particulate organic carbon[135]. The remaining N constituting bulk PN must be heterotrophic bacteria, detrital organic material, and possibly occasional heterotrophic microzooplankton.

The $\delta^{15}N$ of the "sum" can also be calculated (($\delta^{15}N_{Sum} = (\delta^{15}N_{Pro}*N_{Pro} + \delta^{15}N_{Syn}*N_{Syn} + \delta^{15}N_{euk}*N_{euk})/(N_{Pro} + N_{Syn} + N_{euk})$, and includes the $\delta^{15}N$ of heterotrophic bacteria and detritus for the few measurements we have of these pools; fig. S6B and D). In 2008, $\delta^{15}N_{sum}$ was ~0‰, and roughly constant throughout the euphotic zone, whereas in 2009, $\delta^{15}N_{sum}$ was more variable, ranging from -2‰ to 1.5‰. In addition, $\delta^{15}N_{sum}$ for both 2008 and 2009, which represents the average photoautotrophic $\delta^{15}N$, is similar to that of the bulk PN; the high $\delta^{15}N$ of eukaryotes elevates the $\delta^{15}N_{sum}$ only modestly since it is only a modest fraction of the phytoplankton biomass.

Using the [N] and $\delta^{15}N$ of the bulk PN and "sum" pools, we calculate the [N] and $\delta^{15}N$ of the "unmeasured" N, defined as all N pools (e.g., heterotrophic bacteria, detrital organic material etc.) that are not accounted for by our sorted populations ($\delta^{15}N_{unmeas} = (\delta^{15}N_{bulk}*N_{bulk} - \delta^{15}N_{sum}*N_{sum})/(N_{bulk} - N_{sum})$). For both years, $\delta^{15}N_{unmeas}$ is low (-3‰ to 0‰) and similar to bulk PN $\delta^{15}N$, prokaryote $\delta^{15}N$, and $\delta^{15}N_{sum}$. Our few analyses of heterotrophic bacteria and detritus (fig. 2A-B and fig. S6A-B) indicate that these N pools also have a low $\delta^{15}N$ (-1.0‰ and -0.3‰, respectively), which is consistent with their constituting much of the "missing" N in our system

4. Supplemental figures and captions

Figure S1

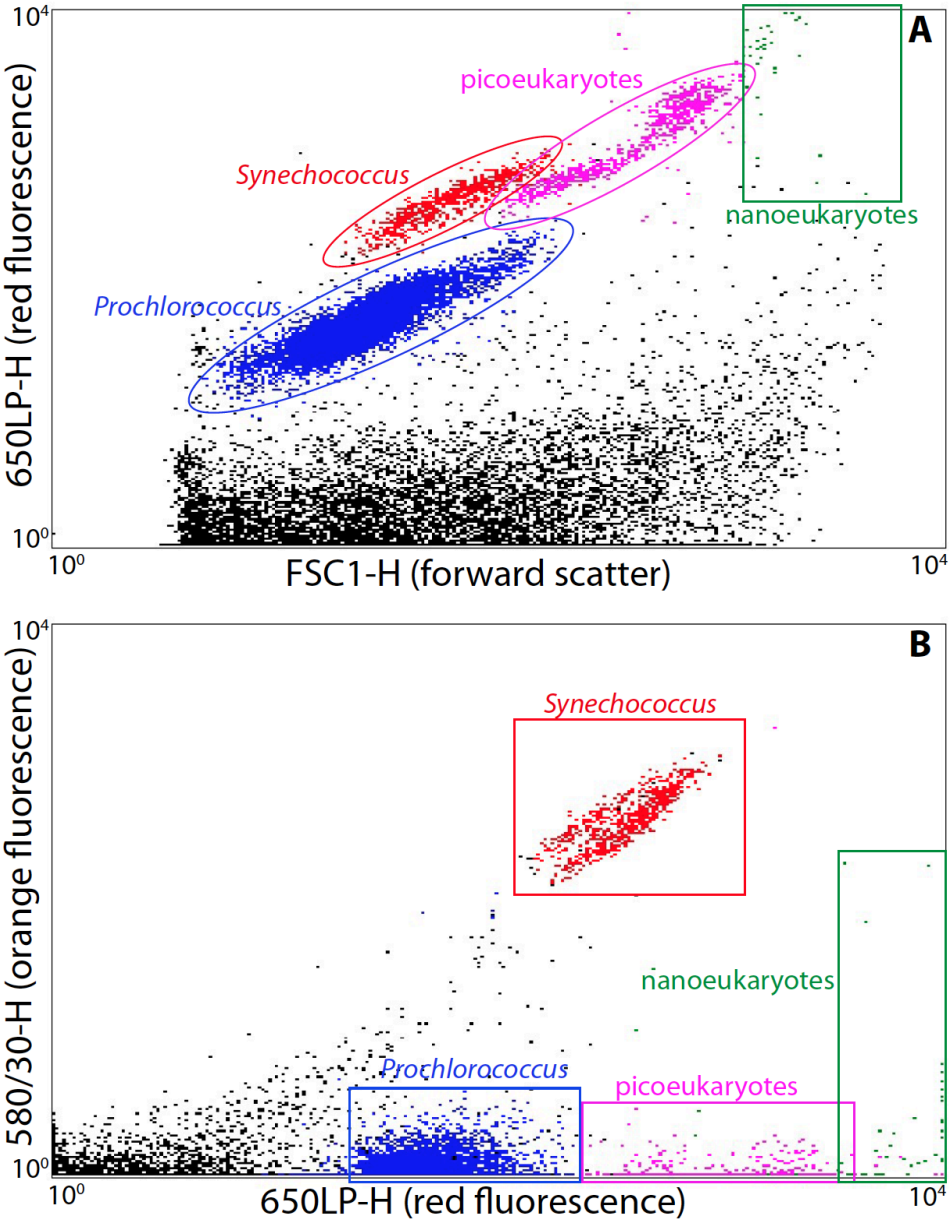

Figure S1: Cytograms representative of the autotrophic populations sorted from collections at BATS in July 2008 and 2009. A) FSC1-H (s-polarized forward scatter) versus 650LP-H (chlorophyll) and B) 650LP-H (chlorophyll) versus 580/30-H (phycoerythrin). Phytoplankton populations of interest (*Prochlorococcus*, *Synechococcus*, and the pico- and nanoeukaryotes that were grouped together as 'eukaryotes') are indicated on the cytograms.

Figure S2

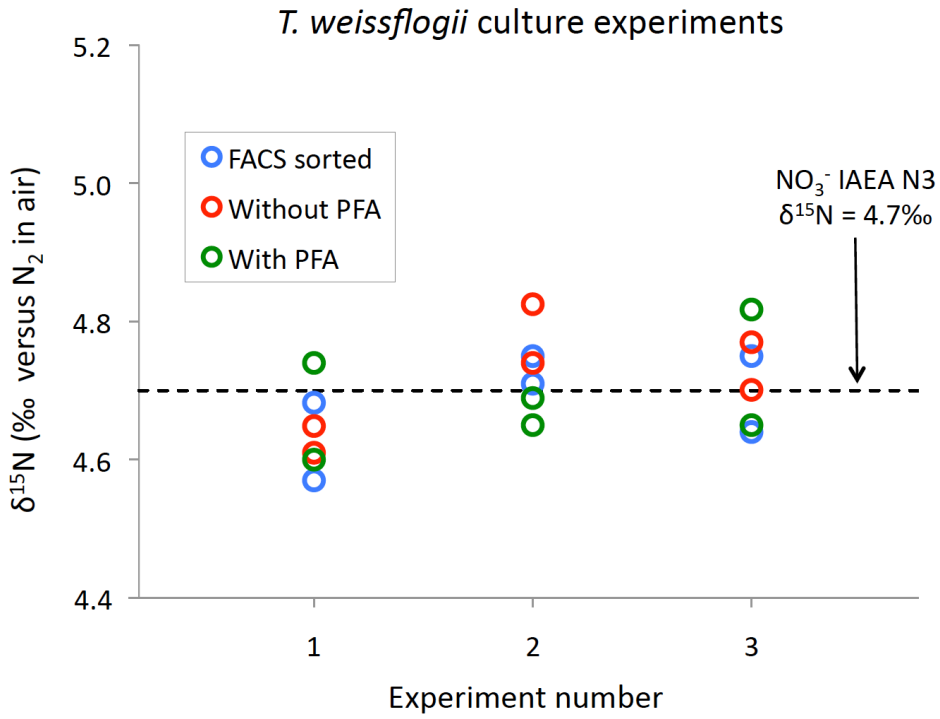

Figure S2: *Thalassiosira weissfloggi* culture experiments conducted to determine the effect on cellular organic N $\delta^{15}N$ of formaldehyde solution (PFA) as the fixative for cells prior to flow cytometric sorting. All experiments (1 – 3) were conducted under the same light and nutrient conditions, with IAEA N3 NO_3^- as the N source to *T. weissfloggi*, since IAEA N3 $\delta^{15}N$ (4.7‰) is well known[62]. "FACS sorted" refers to samples fixed with PFA and then run through the flow cytometer, "without PFA" indicates samples that were not manipulated in any way, and "with PFA" refers to samples that were fixed with PFA but not run through the flow cytometer.

Figure S3:

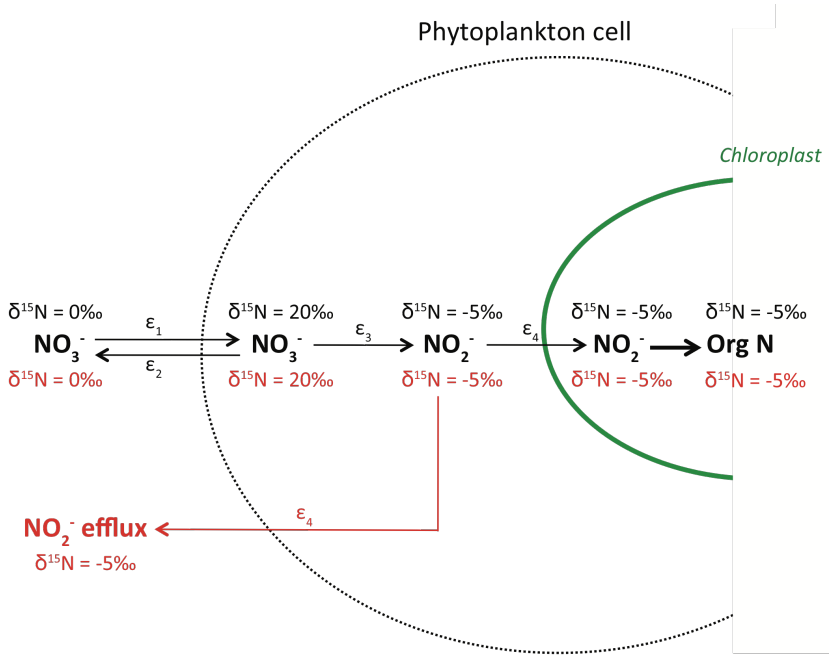

Figure S3: Cartoon showing the isotope systematics associated with the assimilation of nitrate by a eukaryotic phytoplankton cell. Two scenarios are shown: the first assumes all nitrite produced from the reduction of nitrate is assimilated into biomass (Org N; $\delta^{15}N$ values in black), and the second allows for a fraction of this nitrite pool to efflux from the cell (red arrow; $\delta^{15}N$ values in red). The $\delta^{15}N$ values shown in this cartoon apply for the steady state case in which the external nitrate pool is infinite.

Figure S4A-B

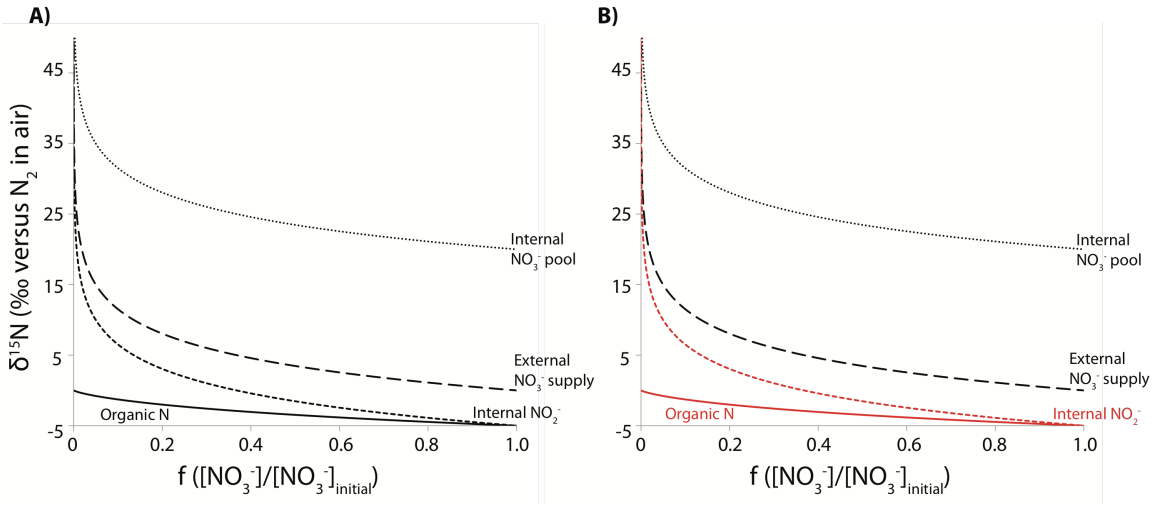

Figure S4A-B: The $\delta^{15}N$ of the same N pools as in fig. S3 above, but for the "Rayleigh" case of the consumption of a finite pool of nitrate. Again, two scenarios are shown: A) assumes all nitrite produced from the reduction of nitrate is assimilated into biomass (organic N), and B) allows for a fraction of this nitrite pool to efflux from the cell (internal NO_2^- and organic N $\delta^{15}N$ shown in red). Note again that the $\delta^{15}N$ of the biomass produced in this scenario is not affected by nitrite efflux. The only difference between the two cases is the amount of organic N that will be produced. In short, the efflux of nitrite is essentially the reversal of the nitrate assimilation steps.

Figure S5

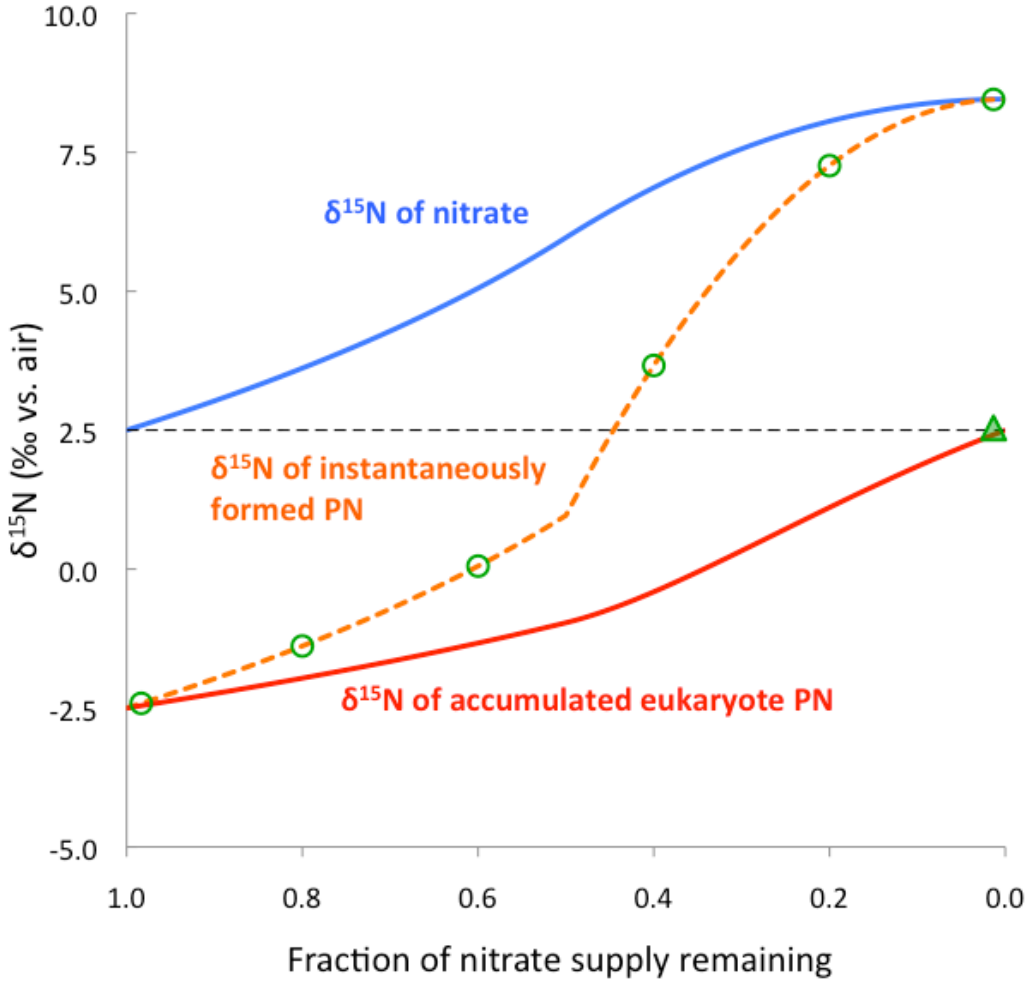

Figure S5: In the Sargasso Sea, thermocline nitrate with a $\delta^{15}N$ of ~2.5‰ is the ultimate source of nitrate to the euphotic zone[50]. As this nitrate supply is consumed by phytoplankton, its concentration decreases and its $\delta^{15}N$ increases (solid blue line) due to isotope discrimination during assimilation. At any instant in time, the $\delta^{15}N$ of PN synthesized from nitrate (dashed orange line) will equal the $\delta^{15}N$ of the nitrate at that same point in time minus any isotope discrimination associated with nitrate assimilation. Integrating over all PN production from nitrate gives a $\delta^{15}N$ of accumulated eukaryote biomass (solid red line) as a function of the amount of nitrate consumed. In the model depicted above, the degree of isotope discrimination is held constant (ε=5‰) until half of the nitrate supply has been consumed, after which ε decreases as a parabolic function of nitrate concentration (ε~0‰ when $[NO_3^-] = 0$ μM). Regardless of the degree of isotope discrimination due to assimilation, or how much it changes during this assimilation, the $\delta^{15}N$ of the accumulated eukaryote PN will always converge on the original $\delta^{15}N$ of the nitrate supply once nitrate has been completely consumed (dashed black line). Individual collections of phytoplankton growing on the supplied nitrate (represented by open green

circles) may fall close to the orange dashed line, since they integrate over only a short period of time and thus perhaps only a short degree of nitrate consumption. Nevertheless, if our samples are not biased in the degree of nitrate consumption that they capture (i.e., they are not clustered around any particular degree of nitrate consumption but rather randomly distributed across this parameter), their integration into a single N pool yields a $\delta^{15}N$ that is similar to the initial $\delta^{15}N$ of the nitrate supply (filled green triangle). Even if individual phytoplankton samples integrate over substantial increments of nitrate assimilation, their averaging still approximates the $\delta^{15}N$ of the initial nitrate supply (calculation not shown).

Figure S6

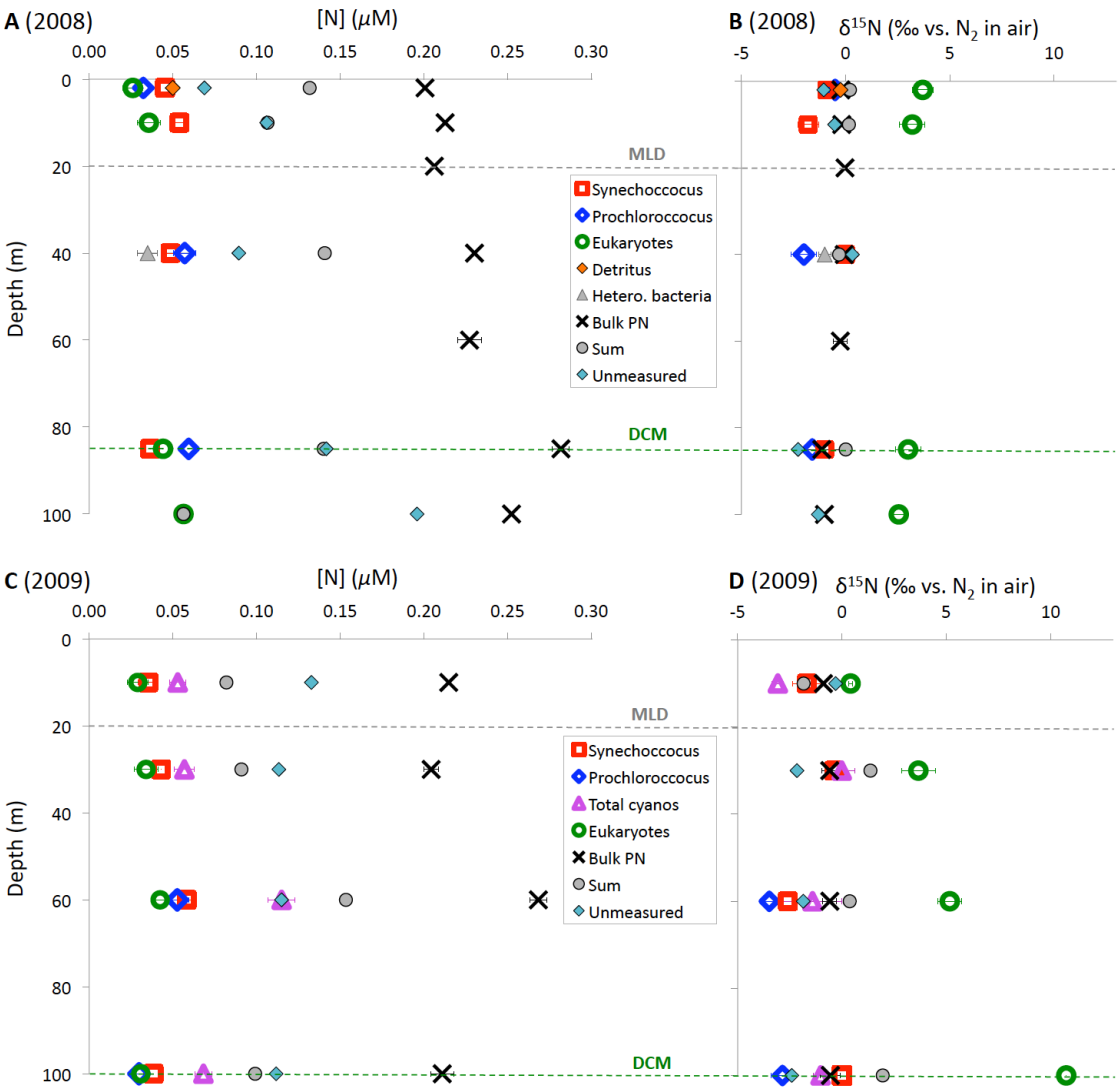

Figure S6: [N] and $\delta^{15}N$ of flow cytometrically sorted components of the PN from the Sargasso Sea in July 2008 (A-B) and 2009 (C-D), as shown in fig. 2a-d. Also included are "Sum" (grey circles), which represents the calculated total [N] and $\delta^{15}N$ of all sorts from a specific depth, and "Unmeasured", which refers to the calculated [N] and $\delta^{15}N$ of bulk PN minus "Sum" PN (i.e., the N fraction not accounted for by the summed sorted populations).

5. Supplemental References

50 Knapp, A. N., Sigman, D. M. & Lipschultz, F. N isotopic composition of dissolved organic nitrogen and nitrate at the Bermuda Atlantic Time-series Study site. *Global Biogeochemical Cycles* **19**, 1-15 (2005).

51 Robinson, R. S., Brunelle, B. G. & Sigman, D. M. Revisiting nutrient utilization in the glacial Antarctic: Evidence from a new method for diatom-bound N isotopic analysis. *Paleoceanography* **19** (2004).

52 Casey, J. R. *et al.* Phytoplankton taxon-specific orthophosphate (Pi) and ATP utilization in the western subtropical North Atlantic. *Aquatic Microbial Ecology* **58**, 31-44 (2009).

53 Guindulain, T., Comas, J. & VivesRego, J. Use of nucleic acid dyes SYTO-13, TOTO-1, and YOYO-1 in the study of *Escherichia coli* and marine prokaryotic populations by flow cytometry. *Appl. Environ. Microbiol.* **63**, 4608-4611 (1997).

54 Kissane, R. J., Tobey, R. A., Crissman, H. A., McLaughlin, S. R. & Kraemer, P. M. Detailed FCM and cell sorting studies on dye-binding kinetics, viability and cell growth of cells following DNA staining with Hoechst-33342. *Cell and Tissue Kinetics* **15**, 105-105 (1982).

55 Herweijer, H., Stokdijk, W. & VIsser, J. W. M. High speed photodamage cell selection using bromodeoxy-uridine/Hoechst 33342 photosensitized cell killing. *Cytometry* **9**, 143-149 (1988).

56 Koroleff, F. in *Methods of Seawater Analysis* Eds K. Grasshoff, M. Ehrhardt, & K. Kremling) 150-157 (Verlag Chemie, 1983).

57 Sigman, D. M. *et al.* A bacterial method for the Nitrogen isotopic analysis of nitrate in seawater and freshwater. *Analytical Chemistry* **73**, 4145-4153 (2001).

58 Casciotti, K. L., Sigman, D. M., Hastings, M. G., Böhlke, J. K. & Hilkert, A. Measurement of the Oxygen isotopic composition of nitrate in seawater and freshwater using the denitrifier method. *Analytical Chemistry* **74**, 4905-4912 (2002).

59 Braman, R. S. & Hendrix, S. A. Nanogram nitrite and nitrate determination in environmental and biological materials by Vanadium(III) reduction with chemi-luminescence detection. *Analytical Chemistry* **61**, 2715-2718 (1989).

60 Garside, C. A chemiluminescent technique for the determination of nanomolar concentrations of nitrate and nitrite in seawater. *Marine Chemistry* **11**, 159-167 (1982).

61 Marie, D., Simon, N. & Vaulot, D. in *Algal Culturing Techniques* (ed R. A. Andersen) p. 596 (Elsevier Academic Press, 2005).

62 Böhlke, J. K. & Coplen, T. B. in *Reference and Intercomparison Materials for Stable Isotopes of Light Elements (IAEA-TECDOC-825)* pp. 51-66 (International Atomic Energy Agency).

63 Moore, L. R. *et al.* Culturing the marine cyanobacterium *Prochlorococcus*. *Limnology and Oceanography: Methods* **5**, 353-562 (2007).

64 Moore, L. R., Post, A. F., Rocap, G. & Chisholm, S. W. Utilization of different nitrogen sources by the marine cyanobacteria *Prochlorococcus* and *Synechococcus*. *Limnology and Oceanography* **47**, 989-996 (2002).

65 Zubkov, M. V., Fuchs, B. M., Tarran, G. A., Burkill, P. H. & Amann, R. High rate of uptake of organic nitrogen compounds by *Prochlorococcus* cyanobacteria as a key to their dominance in oligotrophic oceanic waters. *Appl. Environ. Microbiol.* **69**, 1299-1304 (2003).

66 Zubkov, M. V. & Tarran, G. A. Amino acid uptake of *Prochlorococcus spp.* in surface waters across the South Atlantic Subtropical Front. *Aquatic Microbial Ecology* **40**, 241-249 (2005).

67 Martiny, A. C., Kathuria, S. & Berube, P. M. Widespread metabolic potential for nitrite and nitrate assimilation among Prochlorococcus ecotypes. *Proceedings of the National Academy of Sciences of the United States of America* **106**, 10787-10792 (2009).

68 Casey, J. R., Lomas, M. W., Mandecki, J. & Walker, D. E. *Prochlorococcus* contributes to new production in the Sargasso Sea deep chlorophyll maximum. *Geophysical Research Letters* **34**, 1-5 (2007).

69 Glibert, P. M., Kana, T. M., Olson, R. J., Kirchman, D. L. & Alberte, R. S. Clonal comparisons of growth and photosynthetic responses to nitrogen availability in marine *Synechococcus spp*. *Journal of Experimental Marine Biology and Ecology* **101**, 199-208 (1986).

70 Paerl, H. W. Ecophysiological and trophic implications of light-stimulated amino-acid utilization in marine picoplankton. *Appl. Environ. Microbiol.* **57**, 473-479 (1991).

71 Lindell, D., Padan, E. & Post, A. F. Regulation of ntcA expression and nitrite uptake in the marine *Synechococcus sp.* strain WH 7803. *Journal of Bacteriology* **180**, 1878-1886 (1998).

72 Collier, J. L., Brahamsha, B. & Palenik, B. The marine cyanobacterium *Synechococcus sp.* WH7805 requires urease (urea amidohydrolase, EC 3.5.1.5) to utilize urea as a nitrogen source: molecular, genetic and biochemical analysis of the enzyme. *Microbiology* **145**, 447-459 (1999).

73 Wawrik, B., Callaghan, A. V. & Bronk, D. A. Use of inorganic and organic nitrogen by *Synechococcus spp*. and diatoms on the West Florida shelf as measured using stable isotope probing. *Appl. Environ. Microbiol.* **75**, 6662-6670 (2009).

74 Wyman, M., Gregory, R. P. F. & Carr, N. G. Novel role for phycoerythrin in a marine cyanobacterium, *Synechococcus* Strain Dc2. *Science* **230**, 818-820 (1985).

75 Mulholland, M. R. & Lomas, M. W. in *Nitrogen in the Marine Environment* eds D.G. Capone, D.A. Bronk, M.R. Mulholland, & E.J. Carpenter) Ch. 7, 303 (Elsevier, 2008).

76 Dugdale, R. C. & Goering, J. J. Uptake of new and regenerated forms of nitrogen in primary production. *Limnology and Oceanography* **12**, 196-206 (1967).

77 Menzel, D. W. & Ryther, J. H. The annual cycle of primary production in the Sargasso Sea off Bermuda. *Deep-Sea Research* **6**, 351-367 (1960).

78 Steinberg, D. K. *et al.* Overview of the US JGOFS Bermuda Atlantic Time-series Study (BATS): a decade-scale look at ocean biology and biogeochemistry. *Deep-Sea Research II* **48**, 1405-1447 (2001).

79 Ledgard, S. F., Woo, K. C. & Bergersen, F. J. Isotopic fractionation during reduction of nitrate and nitrite by extracts of spinach leaves. *Australian Journal of Plant Physiology* **12**, 631-640 (1985).
80 Needoba, J. A., Sigman, D. M. & Harrison, P. J. The mechanism of isotope fractionation during algal nitrate assimilation as illuminated by the $^{15}N/^{14}N$ of intracellular nitrogen. *Journal of Phycology* **40**, 517-522 (2004).
81 Collos, Y. Nitrate uptake, nitrite release and uptake, and new production estimates. *Marine Ecology Progress Series* **171**, 293-301 (1998).
82 Lomas, M. W. & Lipschultz, F. Forming the primary nitrite maximum: Nitrifiers or phytoplankton. *Limnology and Oceanography* **51**, 2453-2467 (2006).
83 Kramer, E., Tischner, R. & Schmidt, A. Regulation of assimilatory nitrate reduction at the level of nitrite in *Chlorella Fusca*. *Planta* **176**, 28-35 (1988).
84 Sciandra, A. & Amara, R. Effects of nitrogen limitation on growth and nitrite excretion rates of the dinoflagellate *Prorocentrum Minimum*. *Marine Ecology-Progress Series* **105**, 301-309 (1994).
85 Suzuki, I., Sugiyama, T. & Omata, T. Regulation of nitrite reductase activity under CO_2 limitation in the cyanobacterium *Synechococcus Sp* Pcc7942. *Plant Physiology* **107**, 791-796 (1995).
86 Berges, J. A. & Harrison, P. J. Nitrate reductase activity quantitatively predicts the rate of nitrate incorporation under steady-state light limitation - a revised assay and characterization of the enzyme in 3 species of marine phytoplankton. *Limnology and Oceanography* **40**, 82-93 (1995).
87 Guerrero, M. G., Vega, J. M. & Losada, M. The assimilatory nitrate reducing system and its regulation. *Annual Review of Plant Physiology and Plant Molecular Biology* **32**, 169-204 (1981).
88 Siegel, L. M. & Wilkerson, J. O. in *Molecular and Genetic Aspects of Nitrate Assimilation* (eds J.L. Wray & J.R. Kinghorn) 263-283 (Oxford University Press, 1989).
89 Moore, J. K., Doney, S. C., Glover, D. M. & Fung, I. Y. Iron cycling and nutrient-limitation patterns in surface waters of the World Ocean. *Deep-Sea Research II* **49**, 463-507 (2002).
90 Moore, J. K., Doney, S. C. & Lindsay, K. Upper ocean ecosystem dynamics and iron cycling in a global three-dimensional model. *Global Biogeochemical Cycles* **18** (2004).
91 Prospero, J. M., Ginoux, P., Torres, O., Nicholson, S. E. & Gill, T. E. Environmental characterization of global sources of atmospheric soil dust identified with the Nimbus 7 Total Ozone Mapping Spectrometer (TOMS) absorbing aerosol product. *Reviews of Geophysics* **40** (2002).
92 Sedwick, P. N. *et al.* Iron in the Sargasso Sea (Bermuda Atlantic Time-series Study region) during summer: Eolian imprint, spatiotemporal variability, and ecological implications. *Global Biogeochemical Cycles* **19** (2005).
93 Checkley, D. M., Jr. & Miller, C. A. Nitrogen isotope fractionation by oceanic zooplankton. *Deep-Sea Research* **36**, 1449-1456 (1989).
94 Minagawa, M. & Wada, E. Stepwise enrichment of ^{15}N along food chains - further evidence and the relation between $\delta^{15}N$ and animal age. *Geochimica Et Cosmochimica Acta* **48**, 1135-1140 (1984).

95 Zubkov, M. V. & Tarran, G. A. High bacterivory by the smallest phytoplankton in the North Atlantic Ocean. *Nature* **455**, 224-226 (2008).
96 Arenovski, A. L., Lim, E. L. & Caron, D. A. Mixotrophic nanoplankton in oligotrophic surface waters of the Sargasso Sea may employ phagotrophy to obtain major nutrients. *Journal of Plankton Research* **17**, 801-820 (1995).
97 Sanders, R. W., Berninger, U. G., Lim, E. L., Kemp, P. F. & Caron, D. A. Heterotrophic and mixotrophic nanoplankton predation on picoplankton in the Sargasso Sea and on Georges Bank. *Marine Ecology Progress Series* **192**, 103-118 (2000).
98 Montoya, J. P., Carpenter, E. J. & Capone, D. G. Nitrogen fixation and nitrogen isotope abundances in zooplankton of the oligotrophic North Atlantic *Limnology and Oceanography* **47**, 1617-1628 (2002).
99 Deniro, M. J. & Epstein, S. Influence of diet on the distribution of nitrogen isotopes in animals. *Geochimica Et Cosmochimica Acta* **45**, 341-351 (1981).
100 Lipschultz, F. A time-series assessment of the nitrogen cycle at BATS. *Deep-Sea Research II* **48**, 1897-1924 (2001).
101 DiFiore, P. J., Sigman, D. M. & Dunbar, R. B. Upper ocean nitrogen fluxes in the Polar Antarctic Zone: Constraints from the nitrogen and oxygen isotopes of nitrate. *Geochem. Geophys. Geosyst.* **10** (2009).
102 Hoch, M. P., Fogel, M. L. & Kirchman, D. L. Isotope fractionation associated with ammonium uptake by a marine bacterium. *Limnology and Oceanography* **37**, 1447-1459 (1992).
103 Pennock, J. R., Velinsky, D. J., Ludlam, J. M., Sharp, J. H. & Fogel, M. L. Isotopic fractionation of ammonium and nitrate during uptake by Skeletonema costatum: Implications for $\delta^{15}N$ dynamics under bloom conditions. *Limnology and Oceanography* **41**, 451-459 (1996).
104 Waser, N. A. *et al.* Nitrogen isotope fractionation during nitrate, ammonium and urea uptake by marine diatoms and coccolithophores under various conditions of N availability. *Marine Ecology Progress Series* **169**, 29-41 (1998).
105 Waser, N. A. D., Harrison, P. J., Nielsen, B. & Calvert, S. E. Nitrogen isotope fractionation during the uptake and assimilation of nitrate, nitrite, ammonium, and urea by a marine diatom. *Limnology and Oceanography* **43**, 215-224 (1998).
106 Mariotti, A. *et al.* Experimental determination of nitrogen kinetic isotope fractionation: some principles; illustration for the denitrification and nitrification processes. *Plant and Soil* **62** (1981).
107 Casciotti, K. L., Sigman, D. M. & Ward, B. B. Linking diversity and stable isotope fractionation in ammonia-oxidizing bacteria. *Geomicrobiology Journal* **20**, 335-353 (2003).
108 Granger, J., Sigman, D. M., Lehmann, M. F. & Tortell, P. D. Nitrogen and oxygen isotope fractionation during dissimilatory nitrate reduction by denitrifying bacteria. *Limnology and Oceanography* **53**, 2533-2545 (2008).
109 Bigeleisen, J. Chemistry of Isotopes. *Science* **147**, 463-471 (1965).
110 Hermes, J. D., Weiss, P. M. & Cleland, W. W. Use of ^{15}N and deuterium isotope effects to determine the chemical mechanism of phenylalanine ammonia-lyase. *Biochemistry* **24**, 2959-2967 (1985).

111 Casciotti, K. L. Inverse kinetic isotope fractionation during bacterial nitrite oxidation. *Geochimica et Cosmochimica Acta* **73**, 2061–2076 (2009).
112 Aamand, J., Ahl, T. & Spieck, E. Monoclonal antibodies recognizing nitrite oxidoreductase of *Nitrobacter hamburgensis, N-winogradskyi,* and *N-vulgaris*. *Appl. Environ. Microbiol.* **62**, 2352-2355 (1996).
113 Lipschultz, F., Zafiriou, O. C. & Ball, L. A. Seasonal fluctuations of nitrite concentrations in the deep oligotrophic ocean. *Deep-Sea Research II* **43**, 403-419 (1996).
114 Cochlan, W. P. & Harrison, P. J. Inhibition of nitrate uptake by ammonium and urea in the eucaryotic picoflagellate *Micromonas pusilla* (Butcher) Manton et Parke. *Journal of Experimental Marine Biology and Ecology* **153**, 143-152 (1991).
115 Song, B. K. & Ward, B. B. Molecular cloning and characterization of high affinity nitrate transporters in marine phytoplankton. *Journal of Phycology* **43**, 542-552 (2007).
116 Flores, E. & Herrero, A. Nitrogen assimilation and nitrogen control in cyanobacteria. *Biochemical Society Transactions* **33**, 164-167 (2005).
117 Flores, E., Frias, J. L. E., Rubio, M. & Herrero, A. Photosynthetic nitrate assimilation in cyanobacteria. *Photosynthesis Research* **83**, 117-133 (2005).
118 Dortch, Q., Clayton, J. R., Thoresen, S. S. & Ahmed, S. I. Species differences in accumulation of nitrogen pools in phytoplankton. *Marine Biology* **81**, 237-250 (1984).
119 Eppley, R. W. & Peterson, B. J. Particulate organic matter flux and planktonic new production in the deep ocean. *Nature* **282**, 677-680 (1979).
120 Minagawa, M. & Wada, E. Nitrogen isotope ratios of red tide organisms in the East China Sea - a characterization of biological nitrogen-fixation. *Marine Chemistry* **19**, 245-259 (1986).
121 Johnson, K. S., Riser, S. C. & Karl, D. M. Nitrate supply from the deep to near-surface waters of the North Pacific subtropical gyre. *Nature* **465**, 1062-1065 (2010).
122 McGillicuddy, D. J., Jr. *et al.* Influence of mesoscale eddies on new production in the Sargasso Sea. *Nature* **394**, 263-266 (1998).
123 Jenkins, W. J. & Goldman, J. C. Seasonal oxygen cycling and primary production in the Sargasso Sea. *Journal of Marine Research* **43**, 465-491 (1985).
124 Spitzer, W. S. & Jenkins, W. J. Rates of vertical mixing, gas-exchange and new production - estimates from seasonal gas cycles in the upper ocean near Bermuda. *Journal of Marine Research* **47**, 169-196 (1989).
125 Jenkins, W. J. Studying subtropical thermocline ventilation and circulation using tritium and ^{3}He. *J. Geophys. Res.-Oceans* **103**, 15817-15831 (1998).
126 Jenkins, W. J. Nitrate flux into the euphotic zone near Bermuda. *Nature* **331**, 521-523 (1988).
127 Redfield, A. C., Ketchum, B. H. & Richards, F. A. in *The Sea* Vol. 2 (ed M.N. Hill) Ch. 2, 26-77 (Wiley, 1963).
128 Checkley, D. M. & Entzeroth, L. C. Elemental and isotopic fractionation of carbon and nitrogen by marine, planktonic copepods and implications to the marine nitrogen-cycle. *Journal of Plankton Research* **7**, 553-568 (1985).

129 Altabet, M. A. & Small, L. F. Nitrogen isotopic ratios in fecal pellets produced by marine zooplankton. *Geochimica et Cosmochimica Acta* **54**, 155-163 (1990).
130 Tamelander, T., Soreide, J. E., Hop, H. & Carroll, M. L. Fractionation of stable isotopes in the Arctic marine copepod *Calanus glacialis*: Effects on the isotopic composition of marine particulate organic matter. *Journal of Experimental Marine Biology and Ecology* **333**, 231-240 (2006).
131 Montoya, J. P., Wiebe, P. H. & McCarthy, J. J. Natural abundance of ^{15}N in particulate nitrogen and zooplankton in the gulf-stream region and warm-core ring 86a. *Deep-Sea Research I* **39**, S363-S392 (1992).
132 Altabet, M. A. Variations in nitrogen isotopic composition between sinking and suspended particles: implications for nitrogen cycling and particle transformation in the open ocean. *Deep-Sea Research* **35**, 535-554 (1988).
133 Albertano, P., DiSomma, D. & Capucci, E. Cyanobacterial picoplankton from the central Baltic Sea: cell size classification by image-analyzed fluorescence microscopy. *Journal of Plankton Research* **19**, 1405-1416 (1997).
134 Legendre, L. & Lefevre, J. Microbial food webs and the export of biogenic carbon in oceans. *Aquatic Microbial Ecology* **9**, 69-77 (1995).
135 DuRand, M. D., Olson, R. J. & Chisholm, S. W. Phytoplankton population dynamics at the Bermuda Atlantic Time-series station in the Sargasso Sea. *Deep-Sea Research II* **48**, 1983-2003 (2001).